**Title: S-nitrosothiol signalling is involved in regulating hydrogen peroxide metabolism of zinc-stressed *Arabidopsis***

Kolbert Zs[1]*, Molnár Á[1], Oláh D[1], Feigl G[1], Horváth E[1], Erdei L[1], Ördög A[1], Rudolf E[2], Barth TK[3], Lindermayr C[2]

*1 Department of Plant Biology, University of Szeged, Szeged, Hungary*

*2 Institute of Biochemical Plant Pathology, Helmholtz Zentrum München – German Research Center for Environmental Health, München/Neuherberg, Germany*

*3 Research Unit Protein Science, Helmholtz Zentrum München – German Research Center for Environmental Health, München/Neuherberg, Germany*

Molnár Árpád: molnara@bio.u-szeged.hu

Oláh Dóra: olah.dora18@citromail.hu

Dr. Feigl Gábor: feigl@bio.u-szeged.hu

Dr. Horváth Edit: horvathedo@gmail.com

Dr. Erdei László: erdei@bio.u-szeged.hu

Dr. Ördög Attila: aordog@bio.u-szeged.hu

Eva Rudolf: eva.rudolf@helmholtz-muenchen.de

Dr. Teresa Barth: teresa.barth@helmholtz-muenchen.de

Dr. Christian Lindermayr: lindermayr@helmholtz-muenchen.de

*Corresponding author: Dr. Kolbert Zsuzsanna, kolzsu@bio.u-szeged.hu, +36-30-368-1102

**Date of submission:** 30th Nov 2018

**Number of tables:** 0

**Number of figures:** 8

**Word count:** 6 165

**Number of Supplementary Figures:** 3

**Number of Supplementary Tables:** 4

**Running title: SNO-$H_2O_2$ interplay in zinc-stressed *Arabidopsis***

## Highlight

Zinc-induced $H_2O_2$ regulates its own level due to GSNOR inactivation-triggered SNO signalling affecting APX1.


## Abstract

Accumulation of heavy metals like zinc (Zn) disturbs reactive oxygen (e.g. hydrogen peroxide, $H_2O_2$) and nitrogen species (e.g. nitric oxide, NO; S-nitrosoglutathione, GSNO) metabolism in plant cells; although, their signal interactions are not well understood. Therefore, this study examines the interplay between $H_2O_2$ metabolism and GSNO signalling in *Arabidopsis*. Comparing the Zn tolerance of the wild-type (WT), GSNO reductase (GSNOR) overexpressor *35S::FLAG-GSNOR1* and GSNOR-deficient *gsnor1-3*, we observed relative Zn tolerance of *gsnor1-3* which was not accompanied by altered Zn accumulation capacity. Moreover, in *gsnor1-3* plants Zn did not induce NO/S-nitrosothiol (SNO) signalling possibly due to the enhanced activity of NADPH-dependent thioredoxin reductase. In WT and *35S::FLAG-GSNOR1*, GSNOR was inactivated by Zn and Zn-induced $H_2O_2$ is directly involved in GSNOR activity loss. In WT seedlings, Zn resulted in slight intensification of protein nitration detected by western blot and protein S-nitrosation observed by resin assisted capture of SNO proteins (RSNO-RAC). LC-MS/MS analyses indicate that Zn induces the S-nitrosation of ascorbate peroxidase 1. Our data collectively show that Zn-induced $H_2O_2$ may influence its own level which involves GSNOR inactivation-triggered SNO signalling. These data provide new evidence for the interplay between $H_2O_2$ and SNO signalling in *Arabidopsis* plants affected by metal stress.



**Key words:** excess zinc, *gsnor1-3,* hydrogen peroxide, nitric oxide, S-nitrosoglutathione reductase, S-nitrosothiol, *35S::FLAG-GSNOR1*,

## Introduction

Zinc (Zn) is a non-redox active metal being present in the soils, surface and ground waters (Noulas *et al.,* 2018). Generally, agricultural soils contain 10–300 mg Zn $kg^{-1}$ (with overall mean of 50–55 mg $kg^{-1}$); however, the Zn content of the soils can be enhanced by anthropogenic activities including mining, industrial and agricultural practices (Kiekens, 1995; Zarcinas *et al.,* 2004). Since plants can regulate the absorption of elements within tight limits, in case of large amount of bioavailable Zn in the rhizosphere, the absorbed Zn adversely affects the life processes of plants. Plants grown in the presence of excess Zn have inward-rolled leaf edges, chlorotic leaves, retarded and brownish root system (Sagardoy *et al.,* 2009; Ramankrishna and Rao, 2015; Feigl *et al.,* 2015; 2016). Regarding physiological processes, elevated Zn levels result in perturbations in photosynthesis, glycolysis, electron transport due to the replacement of other divalent cations (Monnet *et al.,* 2001; Lucini and Bernardo, 2015). At the molecular level, a characteristic effect of Zn is the induction of the overproduction of reactive oxygen species (ROS) such as hydroxyl radical ($^{\cdot}OH$), superoxide radical ($O_2^{\cdot-}$) and hydrogen peroxide ($H_2O_2$) as reported by several studies (Weckx and Clijsters, 1997; Jain *et al.,* 2010; Morina *et al.,* 2010; Feigl *et al.,* 2015; 2016). The level of ROS is needed to be strictly regulated by complex mechanisms including several enzymes such as ascorbate peroxidase (APX, EC 1.11.1.11), catalase (CAT, EC 1.11.1.6), superoxide dismutase (SOD, EC 1.1.5.1.1) and non-enzymatic antioxidants like glutathione (GSH) and the activity of these antioxidant components have been shown to be affected by Zn (Cuypers *et al.,* 2002; Di Baccio *et al.,* 2005; Tewari *et al.,* 2008; Gupta *et al.,* 2011; Li *et al.,* 2013). As a result of the Zn-triggered elevation in ROS levels lipids, nucleic acids and proteins can be oxidized. Moreover, Zn stress can be accompanied by impaired DNA repair and poor protein folding (Sharma *et al.,* 2008).

Besides ROS, also reactive nitrogen species (RNS) are formed as the effect of a wide range of environmental stresses including excess Zn (Feigl *et al.,* 2015; 2016). The accumulation of these nitric oxide (NO)-originated molecules principally targets proteins mainly through tyrosine nitration and S-nitrosation (Jain and Bhatla, 2017). Nitration covalently modifies specific tyrosine amino acids in certain proteins yielding 3-nitrotyrosine formation. During the reaction a nitro group is added to one of the two equivalent *ortho* carbons in the aromatic ring of tyrosine residues (Gow *et al.,* 2004) causing steric and electronic perturbations in the protein structure (van der Vliet *et al.,* 1999). In most cases, nitration results in the inhibition of proteins' function in plant systems (Corpas *et al.,* 2013). Moreover, tyrosine nitration possibly can influence signal transduction pathways through the

prevention of tyrosine phosphorylation (Galetskiy *et al.,* 2011). During S-nitrosation, RNS react with the thiol group of cysteine (Cys) resulting in the formation of S-nitrosothiol (SNO) group which in turn causes alterations in protein structure and function (Lamotte *et al.,* 2015). So far more than a dozen proteins have been found to be regulated either positively or negatively by S-nitrosation (reviewed by Zaffagnini *et al.,* 2016). The S-nitrosation reaction affects also GSH yielding S-nitrosoglutathione (GSNO) which has particular relevance due to its highly stable character, its capability for being transported and its ability to liberate NO. Based on these, GSNO is considered to be mobile reservoir of NO (Umbreen *et al.,* 2018). The intracellular level of GSNO and consequently the intensity of SNO signalling is controlled by direct and selective processes like NADPH-dependent thioredoxin reductase (NTR)-thioredoxin (TRX) system (Kneeshaw *et al.,* 2014; Umbreen *et al.,* 2018) and also by GSNO reductase activity (GSNOR, EC 1.2.1.1, Feechan *et al.,* 2005; Lee *et al.,* 2008; Chen *et al.,* 2009). The latter enzyme catalyses the NADH-dependent conversion of GSNO to GSSG and $NH_3$. The GSNOR enzyme locates in the cytosol, chloroplasts, mitochondria and possibly also in the peroxisomes (Chaki *et al.,* 2011; Ticha *et al.,* 2017) and it is coded by a single gene (At5g43940). Regarding its protein structure, GSNOR is rich in Cys residues and contains two Zn ions per subunit, one of which has catalytic the other has structural role (Lindermayr, 2018). Recently, a direct interaction between $H_2O_2$ and GSNOR enzyme was revealed where the $H_2O_2$ inducer (paraquat) triggered catalytic $Zn^{2+}$ release from the protein leading to inactivation of the enzyme (Kovács *et al.,* 2016). As a consequence of GSNOR inhibition, SNO accumulated and S-nitrosation intensified suggesting a direct link between ROS and GSNO homeostasis. Since ROS overproduction can be observed during diverse environmental stresses, we can suppose that this signal interaction between ROS and RNS can be a general mechanism regulating stress responses in plants. To test this hypothesis, Zn as an environmental stressor was applied and the alterations and connections in ROS and RNS metabolism were examined. We focused our work on GSNO metabolism therefore in a genetic approach we applied GSNOR deficient mutant (*gsnor1-3*) and overproducer transgenic line (*35S::FLAG-GSNOR1*).

## Materials and methods

### Plant material and growth conditions

Seven-days-old wild-type (*Col-0*, WT), *35S::FLAG-GSNOR1* (Frungillo *et al.*, 2014) and *gsnor1-3* (At5g43940, Chen *et al.*, 2009) *Arabidopsis thaliana* L. seedlings in *Col-0* background were used. The seeds were surface sterilized with 70% (v/v) ethanol and 5% (v/v) sodium hypochlorite and transferred to half-strength Murashige and Skoog medium (1% (w/v) sucrose and 0.8% (w/v) agar) supplemented with 250 µM zinc sulphate ($ZnSO_4$). In case of control Petri dishes, the media contained 15 µM $ZnSO_4$ as indicated by the manufacturer (Duschefa Biochemie). The Petri dishes were kept vertically in a greenhouse at a photo flux density of 150 µmol $m^{-2}$ $s^{-1}$ (8/16 day/night period) at a relative humidity of 55-60% and 25 ± 2°C. As an exogenous treatment, 1 mM GSH was added to 4-days-old seedlings through sterile filter.

### Evaluation of Zn tolerance

Length of primary roots were measured and from the data Zn tolerance index (%) was calculated according to the following formula: tolerance index (%)= (treated root length/mean control root length) * 100. Additionally, fresh weights of 10 seedlings were measured and the data are presented as average seedling fresh weight (mg $seedling^{-1}$). These data were acquired from three separate generations, and in each generation 20 plants were examined (n=20).

### Enzyme activity assays

Whole seedlings of WT, *35S::FLAG.GSNOR1* and *gsnor1-3 Arabidopsis* were grounded with double volume of extraction buffer (50 mM Tris–HCl buffer pH 7.6–7.8) containing 0.1 mM EDTA, 0.1% Triton X-100 and 10% glycerol and centrifuged at 9 300 g for 20 min at 4°C. The protein extract was treated with 1% protease inhibitor cocktail and stored at -20 °C. Protein concentration was determined using the Bradford (1976) assay with bovine serum albumin as a standard.

GSNOR activity was determined by monitoring NADH oxidation in the presence of GSNO at 340 nm (Sakamoto *et al.*, 2002). Plant homogenate was centrifuged at 14 000 g for 20 min at 4 ºC and 100 µg of protein extract was incubated in 1 mL reaction buffer containing

20 mM Tris-HCl pH 8.0, 0.5 mM EDTA, 0.2 mM NADH. Data are expressed as nmol NADH $min^{-1}$ $mg^{-1}$ protein.

The activity of APX was measured by monitoring the decrease of ascorbate (Asc) content at 265 nm according to the modified method of Nakano and Asada (1981). For the enzyme extract, 250 mg of plant material was grounded with 1.5 mL of extraction buffer containing 1 mM EDTA, 50 mM NaCl, 900 mM Asc and 1 % polyvinylpyrrolidone (PVP). Data are expressed as activity (unit $g^{-1}$ fresh weight).

CAT enzyme activity was measured as described by Kato and Shimizu (1987). For the enzyme extract, 250 mg of plant material was grounded with 10 mg of polyvinyl polypyrrolidone (PVPP) and 1 mL of 50 mM phosphate buffer (pH 7.0, with 1mM EDTA added). The measurement itself quantifies the degradation of $H_2O_2$ at 240 nm. The data are shown as unit $g^{-1}$ fresh weight.

SOD activity was determined by measuring the ability of the enzyme to inhibit the photochemical reduction of nitroblue tetrazolium (NBT) in the presence of riboflavin in light (Dhindsa *et al.,* 1981). The same enzyme extract was used as described previously. The enzyme activity is expressed as unit $g^{-1}$ fresh weight; 1 unit of SOD corresponds to the amount of enzyme causing a 50 % inhibition of NBT reduction in light. For the examination of SOD isoenzyme activities, the protein extract was subjected to native gel electrophoresis on 10 % polyacrylamide gel (Beauchamp and Fridovich, 1971). The gel was incubated for 20 minutes in 2.45 mM NBT in darkness then for 15 minutes in freshly prepared 28 mM TEMED solution containing 2.92 µM riboflavin. After the incubation, the gels were washed two times and developed by light exposure. SOD isoforms were identified by incubating gels in 50 mM potassium phosphate containing 2 mM potassium cyanide to inhibit Cu/Zn SOD activity or 5 mM $H_2O_2$ which inhibits Cu/Zn and Fe SOD activity for 30 min before staining with NBT. Mn SODs are resistant to both inhibitors. To evaluate native electrophoresis silver staining was performed according to Blum *et al.* (1987) with slight modifications. The gel was fixed with methanol and acetic acid, then treated with a sensitizing solution and staining solution containing $AgNO_3$. The gel was developed in a solution containing sodium carbonate and formaldehyde.

The activity of NTR was measured based on the method of Arnér *et al*. (1999) using a kit (Thioredoxin Reductase Assay Kit, Sigma-Aldrich). The manufacturer's instructions were followed during the procedure and the protein extract was prepared as described above. The measurement is based on a colorimetric reduction of 5,5'-dithiobis-2-nitrobenzoic acid (DTNB) to a yellow colour 5-thio-2-nitrobenzoic acid with NADPH. To ensure selectivity, a

specific NTR inhibitor was used and to validate data rat liver thioredoxin reductase was used as positive control. Data are shown as unit µg protein$^{-1}$. These experiments were carried out on two separate plant generations with five samples in each (n=5).

The measurement of total GSH content was done according to Tari *et al.* (2015) with slight modifications. Whole seedlings were grounded with 5% trichloroacetic acid and centrifuged for 20 min at 9 300 g and the supernatant was used for further measurement. The reaction mixture contained 25 µl sample, 0.1 M sodium phosphate buffer, 1 mM of DTNB, 1 mM NADPH and 1 U of glutathione reductase enzyme. Data are shown as nmol g$^{-1}$ fresh weight. These experiments were carried out on two separate plant generations with five samples in each (n=5).

**Microscopic detection of Zn levels, NO, $H_2O_2$ and $O_2^{\cdot-}$ in the roots**

The endogenous levels of Zn were visualized by the Zn-specific fluorophore, Zinquin (ethyl (2-methyl-8-p-toluenesulphonamide-6-quinolyloxy)acetate (Helmersson *et al.*, 2008). Seedlings were equilibrated in phosphate-buffered saline (PBS; 137 mM NaCl, 2,68 mM KCl, 8.1 mM $Na_2HPO_4$, 1.41 mM $KH_2PO_4$, pH 7.4) and further incubated in 25 µM Zinquin solution (in PBS) for 60 min at room temperature in darkness. Before the microscopic investigation the samples were washed once with PBS buffer.

Nitric oxide levels of the root tips were monitored with the help of 4-amino-5-methylamino- 2′,7′-difluorofluorescein diacetate (DAF-FM DA) according to Kolbert *et al.* (2012). Whole seedlings were incubated in 10 µM dye solution for 30 min (darkness, 25±2 $^{o}$C), and washed twice with Tris-HCl (10 mM, pH 7.4).

The levels of $H_2O_2$ were detected by Amplex Red (AR) which in the presence of peroxidase and $H_2O_2$ forms highly fluorescent resorufin (Prats *et al.*, 2008). Seedlings were incubated in 50 µM AR solution (prepared in sodium phosphate buffer pH 7.5) for 30 min at room temperature in darkness. The microscopic observations were preceded by one washing step with sodium phosphate buffer.

Dihydroethidium (DHE) at 10 µM concentration was applied for the detection of superoxide anion levels in the roots. Seedlings were incubated for 30 min in darkness at 37 $^{o}$C, and washed two times with Tris-HCl buffer (10 mM, pH 7.4) (Kolbert *et al.*, 2012).

Seedlings labelled with different fluorophores were examined under Zeiss Axiovert 200 M microscope (Carl Zeiss, Jena, Germany) equipped with filter set 9 (excitation 450-490 nm, emission 515-∞ nm) for DHE, filter set 10 (excitation 450-490 nm, emission 515-565

nm) for DAF-FM DA, filter set 20 HE (excitation 546/12 nm, emission 607/80 nm) for Amplex Red or filter set 49 (excitation 365 nm, emission 455/50 nm) for Zinquin. Fluorescence intensities (pixel intensity) in the roots were measured on digital images using Axiovision Rel. 4.8 software within circles of 37 µm radii. These analyses were carried out three times with 10 samples each (n=10).

**Determination of SNO contents**

The total amount of SNO was quantified by Sievers 280i NO analyser (GE Analytical Instruments, Boulder, CO, USA). 250 mg of *Arabidopsis* seedlings were mixed with double volume of PBS buffer and were grounded using Fast Prep ® Instrument (speed 5.5; 60 s, Savant Instruments Inc., Holbrook, NY). Samples were centrifuged twice for 15 min, at 20 000 g at 4 ºC each. The supernatants were incubated with 20 mM sulphanilamide (prepared in 1M HCl) at the ratio of 9:1 in order to remove nitrite. 250 µL of the samples were injected into the reaction vessel filled with potassium iodide. SNO concentrations were quantified with the help of NO analysis software (v3.2) by integrating peak areas and using a standard curve. Standard curve was generated by adding known concentrations of sodium nitrite. These experiments were carried out on three separate plant generations with 5-7 samples examined each (n=5-7).

**Analysis of S-nitrosylated proteins by RSNO-RAC**

For the determination of S-nitrosylated proteins in wild-type *Arabidopsis* seedlings, the method of resin-assisted capture of SNO proteins was adapted (Thompson *et al.*, 2013). Whole seedling material (2 g) were grounded in liquid nitrogen and homogenized in HENT buffer (100 mM HEPES-NaOH, pH 7.4, 1 mM EDTA, 0.1 mM neocuproine, 0.2% Triton X-100). The homogenate was centrifuged at 18 000 g, 15 min, 4 ºC followed by another centrifugation step (18 000 g, 10 min, 4 ºC). Protein concentration was determined according to Bradford (1976). Some of the samples were treated with 1 mM GSNO for 30 min in the darkness with multiple mixes. During the blocking step, samples were incubated with 25 % SDS and 2 M MMTS at 50 ºC, at 300 rpm, for 20 min. Incubation of the samples with 100% ice cold acetone at -20 ºC was followed by several washings with 70% acetone with centrifugations (5 min, 10 000 g). The pellets were re-suspended in HENS buffer (HEN+1% SDS) and input controls were mixed with Laemmli 2x. Certain samples were treated with 200 mM sodium Asc for 10 min. The previously prepared Thiopropyl sepharose 6B (GE Healthcare Life Sciences) beads were added to the samples and those were incubated with the

beads for 2 hours in the darkness with a constant mixing. The beads were washed with 4x3 ml HENS buffer and 2x2 ml HENS/10 buffer. Elution of the samples were carried out with mercaptoethanol. Samples were subjected to SDS-PAGE (12%) and the gels were stained with Coomassie Brilliant Blue R-350 (input controls) or with silver (Pierce™ Silver Stain Kit, Thermo Fisher Scientific). These analyses were carried out on three separate plant generations (n=3).

**Sample Preparation for MS Analysis**

From each of the SNO-enriched purifications, a part of the eluted proteins was digested using a modified filter-aided proteome preparation procedure (Wiśniewski *et al.*, 2009). The samples were acidified with trifluoroacetic acid and stored at −20°C.

**Mass Spectrometry**

LC-MS/MS analysis was performed on a Q Exactive HF mass spectrometer (Thermo Fisher Scientific) online coupled to a nano-RSLC (Ultimate 3000 RSLC; Dionex). Tryptic peptides were accumulated on a nano trap column (Acclaim PepMap 100 C18, 5 µm, 100 Å, 300 µm inner diameter (i.d.) × 5 mm; Thermo Fisher Scientific) at a flow rate of 30 µl $min^{-1}$ and then separated by reversed phase chromatography (nanoEase M/Z HSS C18 T3 Column, 100Å, 1.8 µm, 75 µm i.d. x 250 mm; Waters) using a non-linear gradient for 95 minutes from 3 to 40% buffer B (acetonitrile [v/v]/0.1% formic acid [v/v]) in buffer A (2% acetonitrile [v/v]/0.1% formic acid [v/v] in HPLC-grade water) at a flow rate of 250 nl $min^{-1}$. MS spectra were recorded at a resolution of 60,000 with an AGC target of 3 x 106 and a maximum injection time of 50 ms at a range of 300 to 1500 m/z. From the MS scan, the 10 most abundant ions were selected for HCD fragmentation with a normalized collision energy of 28, an isolation window of 1.6 m/z, and a dynamic exclusion of 30 s. MS/MS spectra were recorded at a resolution of 15 000 with an AGC target of 105 and a maximum injection time of 50 ms. Unassigned charges, and charges of 1 and >8 were excluded.

**Label-Free Analysis**

The acquired spectra were loaded into the Progenesis QI for proteomics software (version 4.0; Nonlinear Dynamics) for MS1 intensity based label-free quantification. Alignment of retention times was performed to a maximal overlay of all features. After exclusion of features with one charge and charges >7, all remaining MS/MS spectra were exported as Mascot generic file and used for peptide identification with Mascot (version

2.6.2) with the TAIR database (Release 10, 35386 entries). Search parameters used for Mascot search were 10 ppm peptide mass tolerance and 20 mmu fragment mass tolerance with trypsin as protease and one missed cleavage allowed. Carbamidomethylation of cysteine was set as fixed modification, methionine oxidation and asparagine or glutamine deamidation were allowed as variable modifications. Mascot integrated decoy database search was set to a false discovery rate (FDR) of 5%. Peptide assignments were reimported into the Progenesis QI software. Raw protein abundances resulting from the addition of all unique peptides of a given protein group were used for calculation of +Asc/–Asc ratios for each protein and each replicate. Proteins with a ratio higher than at least 1.2 in each replicate were defined as S-nitrosated.

**qRT-PCR analysis**

The expression rate of *GSNOR1* and *THIOREDOXIN-h3* (*TRXh3)* genes in *Arabidopsis thaliana* was determined by quantitative real-time reverse transcription-PCR (RT-qPCR). RNA was purified from 90 mg plant material by using NucleoSpin RNA Plant mini spin kit (Macherey-Nagel) according to the manufacturer's instruction. An additional DNase digestion was applied (Thermo Fisher Scientific), and cDNA was synthetized using RevertAid reverse transcriptase (Thermo Fisher Scientific). Primers were designed for the selected coding sequences using the Primer3 software; the primers used for RT-qPCR are listed in Table S1. The expression rate of the selected genes was monitored by quantitative real-time PCR (qRT-PCR, Jena Instruments) using SYBR Green PCR Master Mix (Thermo Scientific) as described by Gallé *et al.* (2009). Data analysis was performed using qPCRsoft3.2 software (Jena instruments). Data were normalised to the transcript levels of the control samples; *ACTIN2* (*At3g18780*) and *GAPDH2* (*At1g13440*) were used as internal controls (Papdi *et al.*, 2008). Each reaction was carried out in two replicates using cDNA synthesised from independently extracted RNAs and the experiments were repeated two times.

**Western blots analyses of proteins**

Protein extracts were prepared as described above. 15 µl of denaturated protein extract was subjected to SDS-PAGE on 12 % acrylamide gels. Transfer to PVDF membranes was done using a wet blotting procedure (25 mA, 16 h) and membranes were used for cross reactivity assays with different antibodies. To evaluate the electrophoresis and transfer, we

used Coomassie Brilliant Blue R-350 staining according to Welinder and Ekblad (2011). As a protein standard, actin from bovine muscle (Sigma-Aldrich, cat. No. A3653) was used.

Immunoassay for GSNOR enzyme was performed using a polyclonal primary antibody from rabbit (Agrisera, cat. No. AS09 647) diluted 1:2000. As secondary antibody affinity-isolated goat anti-rabbit IgG–alkaline phosphatase secondary antibody was used (Sigma-Aldrich, cat. No. A3687) at a dilution of 1:10 000, and bands were visualized by using the NBT/BCIP (5-bromo-4-chloro-3-indolyl phosphate) reaction.

To evaluate APX protein content western blot using rabbit anti-APX antibody (Agrisera, cat. No. AS 08 368) was used. As secondary antibody, similarly to previous methods goat anti-rabbit IgG–alkaline phosphatase was used. Development was performed with the NBT/BCIP reaction.

Detection of nitrated proteins were similar as described above. Membranes were subjected to cross-reactivity assay with rabbit polyclonal antibody against 3-nitrotyrosine (Sigma-Aldrich, cat. No. N0409) diluted 1:2000. As secondary antibody affinity-isolated goat anti-rabbit IgG–alkaline phosphatase secondary antibody was used (Sigma-Aldrich, cat. No. A3687) at a dilution of 1:10 000, and bands were visualized by using the NBT/BCIP reaction. For positive control nitrated BSA (Sigma-Aldrich, cat. No. N8159) was used. Protein bands of nitrated protein, GSNOR enzyme and APX enzyme were quantified by Gelquant software (provided by biochemlabsolutions.com). Western blot was applied to two separate protein extracts from different plant generations, multiple times per extract, giving a total of four blotted membranes (n=2).

**Statistical analysis**

All results are shown as mean values of raw data (±SE). For statistical analysis, Duncan's multiple range test (One-way ANOVA, $P \leq 0.05$) was used in SigmaPlot 12. For the assumptions of ANOVA we used Hartley's $F_{max}$ test for homogeneity and Shapiro-Wilk normality test.

## Results and discussion

### GSNOR-deficient line tolerates exogenous Zn better than the wild-type and *35S::FLAG-GSNOR1*

In pilot experiments, 7-days-long, 250 µM Zn treatment was chosen, since this concentration during this period proved to be non-toxic for the plant lines. As the effect of Zn, the fresh weight of seedlings decreased in the WT and GSNOR overproducer line, but was not influenced in *gsnor1-3* (Fig 1A). However, it has to be noted that the *gsnor1-3* mutant shows multiple developmental arrests compared to the WT (Fig 1C, Lee *et al.,* 2008, Holzmeister *et al.,* 2011, Kwon *et al.,* 2012). The semidwarf phenotype of *gsnor1-3* indicates that the GSNOR-dependent NO removal is necessary for optimal development. In case of the WT and *35S::FLAG-GSNOR1* plants, the tolerance index decreased as the effect of Zn (Fig 1BC) which together with reduced biomass indicates Zn sensitivity. Moreover, the most significant Zn-triggered biomass loss (44%) and root shortening (20%) was observed in the GSNOR overexpressor line (Fig 1 ABC). Interestingly, Zn tolerance index of *gsnor1-3* was increased which suggests relative Zn tolerance of this mutant. Similarly, the *gsnor1-3* mutant shows selenium and copper tolerance (Lehotai *et al.,* 2012, Pető *et al.,* 2013); although in case of this mutant impaired disease resistance and reduced heat tolerance has been observed (Feechan *et al.,* 2005, Lee *et al.,* 2008). This implies the possibility that the role of SNO signalling can regulate stress responses positively or negatively depending on the nature of the stress.

### Zn accumulation and its root-level distribution is similar in all plant lines

In order to examine whether the different Zn tolerance of the lines is associated with different Zn accumulation capacity, Zn levels were detected using *in situ* and *in vivo* microscopy. All three plant lines were able to take up Zn from the medium which was confirmed by the elevated Zn-specific fluorescence both in the meristematic and in the differentiation root zones (Fig 2). In the presence of 250 µM Zn, the degree and the magnitude of Zn accumulation proved to be similar in *gsnor1-3* to the WT and *35S::FLAG-GSNOR1* roots (Fig 2). This suggests that the reason for the relative Zn tolerance of *gsnor1-3* is not the low Zn uptake capacity.

### Zn negatively regulates GSNOR activity without decreasing protein abundance and gene expression

As expected, under control conditions, both the GSNOR activity (Fig 3A) and the protein abundance (Fig 3B) was elevated in the overexpressor *35S::FLAG-GSNOR1* line and

reduced in the *gsnor1-3* line relative to the WT. Excess Zn resulted in the significant reduction in the GSNOR activity in the WT and caused a highly significant activity loss in the *35S::FLAG-GSNOR1* line which was comparable with the effect of the GSNOR mutation (Fig 3A). The decrease in GSNOR activity was not accompanied by the reduction in protein abundance, suggesting that most of the GSNOR enzyme pool present in the Zn-treated plant may be inactive. The relative transcript level of GSNOR1 was influenced by Zn treatment neither in the WT nor in the mutant lines (Fig 3C) indicating that the Zn-induced changes in GSNOR activity may occur at the post-transcriptional level.

**NADPH-dependent thioredoxin reductase system regulates SNO levels in Zn-treated *gsnor1-3***

Compared to the WT, the NO level in *35S::FLAG-GSNOR1* roots was two times higher (Fig 4A) which can be explained by the higher nitrate content and increased nitrate reductase (NR) activity of this line (Frungillo *et al.,* 2014). As a consequence of GSNOR overproduction, the SNO levels of *35S::FLAG-GSNOR1* were lower than in the WT seedlings under control conditions (Fig 4B). Both the NO and SNO levels of WT plants were increased by Zn indicating intensified S-nitrosation processes. Zn treatment caused decreased NO levels in the root of GSNOR oveerexpressor *35S::FLAG-GSNOR1*, but the resulting NO content was comparable with the NO level of the Zn-treated wild-type. As for the SNO levels, those increased in Zn-exposed *35S::FLAG-GSNOR1* seedlings similarly to the WT. Several processes can be hypothesized in the background of Zn-induced NO level changes. Zn-induced iron-deficiency can be partially responsible for NO production in *Arabidopsis* seedlings as it was observed in *Solanum nigrum* root tips (Xu *et al.,* 2010). Additionally, the major enzymatic source of NO in the root system is NR but the expressions of *NIA1* or *NIA2* were not modified by Zn (data not shown) and the activity of NR was not influenced by Zn in *Brassica* roots (Bartha *et al.,* 2005). One possibility for the NO production in this system is the metal-triggered decomposition of GSNO but this remains to be elucidated. The roots of the control *gsnor1-3* mutant showed increased NO level (Fig 4A) and slightly elevated total SNO level (Fig 4B) compared to the WT, which may be the result of the more than 80% loss of GSNOR activity (Lee *et al.,* 2008, Fig 3A). Zn did affect neither NO nor SNO levels in the *gsnor1-3* mutant, which is interesting because in the absence of GSNOR activity, a GSNOR-independent mechanism is necessary to prevent SNO and NO production. Besides GSNOR, the NADPH-NTR-TRX system has been considered as direct and selective denitrosylases (Umbreen *et al.,* 2018) maintaining low SNO levels and thus temporally and spatially limiting

SNO signalling. Therefore, NTR-TRX system is a good candidate for preventing Zn-induced NO/SNO level increase in case of GSNOR deficiency. Indeed, Zn increased the activity of NTR in *gsnor1-3* seedlings (Fig 4C). Additionally, in the WT and *35S::FLAG-GSNOR1*, NTR activity was lowered by Zn exposure which together with Zn-triggered GSNOR inactivation contributes to the intensification of SNO signalling. Examining the expression of *TRX*s (Fig 4D), we found that the expression of *TRXh3* is induced by Zn in the WT but not in the other lines and Zn did influence the expression of *TRXh5* in none of the examined *Arabidopsis* lines (data not shown). However, it cannot be excluded that TRX activity is regulated post-transcriptionally in Zn-stressed plants. These data collectively point out that Zn intensifies SNO signalling in the WT and GSNOR overproducer line, while in case of GSNOR deficiency the induction of NTR activity may be involved in limiting SNO signalling in the presence of Zn.

**Zn induces S-nitrosation in wild-type *Arabidopsis* seedlings**

The enhancement of total SNO levels predicted the possible intensification of protein S-nitrosation in Zn-treated *Arabidopsis*. Therefore, protein extracts derived from wild-type *Arabidopsis* seedlings were subjected to RSNO-RAC method in order to compare the rate of S-nitrosation in the seedlings grown in the presence of optimal or supraoptimal Zn supply. To verify the method, the protein extract was incubated in the presence of GSNO with the addition of Asc (Fig 5A). In this sample, a remarkable enrichment of SNO proteins was observed, while in the absence of Asc much less SNO-proteins were detected (Fig 5A). These controls confirm for the first time the usability of the method for detecting SNO-proteins in plant systems. Regarding the Zn effect, a slightly intensified S-nitrosation could be detected compared to the control conditions possibly due to the moderate nature of Zn exposure (250 µM). To identify protein candidates for Zn-induced S-nitrosation, the samples were analysed also by LC-MS/MS. In case of GSNO treatment (*in vitro* S-nitrosation), 69 protein candidates were identified (Table S2) while *in vivo* S-nitrosation in control seedlings affected 26 proteins (Table S3). In Zn-treated seedlings, 18 proteins were found to be S-nitrosylated which are listed in Fig 5B. Among them the S-nitrosation of APX1 was induced exclusively by the presence of Zn. According to the literature, the S-nitrosation modification of APX1 occurs at Cys32 and leads to the activation of the enzyme (Begara-Morales *et al.*, 2014, Yang *et al.*, 2015). In case of measuring the total activity of APX isoforms; however, we observed significant (~40%) Zn-induced activity loss (Fig 5C). Moreover, 250 µM Zn treatment caused decrease in APX protein level of WT and *gsnor1-3* seedlings, while in GSNOR-overproducer

plants it seemed to be less modified (Fig 5E and Fig S2). These suggest that Zn affects APX activity by lowering protein content in WT and GSNOR-deficient plants; however, GSNOR overproduction prevents the loss of APX protein level and causes inactivation without significantly influencing protein abundance.

Catalase (CAT 3) was identified as a target for S-nitrosation in GSNO-treated samples (Table S2), therefore the total activity of isoforms was measured in control and Zn-treated seedlings (Fig 5D). Zinc reduced CAT activities in all three plant lines; however, in case of *gsnor1-3* the activity loss was not statistically significant. It is worth noting that control *35S::FLAG-GSNOR1* seedlings had four-fold CAT activity compared to the WT (Fig 5D) suggesting an effective $H_2O_2$ detoxification system in case of intensified SNO signalling. The reason for the significant (~40-50%) activity losses of APX and CAT may be, *inter alia*, protein nitration, since both enzymes have previously been shown to be nitrated (Begara-Morales *et al.*, 2014, Chaki *et al.*, 2015).

**Zn-induced $H_2O_2$ is directly involved in GSNOR inactivation**

In Zn-exposed plants, SNO signalling affected $H_2O_2$-associated enzymes (Fig 5), therefore it could be suspected that $H_2O_2$ levels are modified by the presence of Zn. Indeed, Zn treatment resulted in elevated $H_2O_2$ levels in the root system of all three plant lines; although this induction was the most intense (9-fold) in *gsnor1-3* compared to the WT and GSNOR overexpressor line (1.5-fold, Fig 6A). Despite the WT-like APX and CAT activities, the GSNOR-deficient line contained only 20% of the $H_2O_2$ levels of the WT in its root system under control conditions. This low $H_2O_2$ level may be associated with the significantly (3-fold) increased total GSH content of this line (Fig 6B). Kovács *et al.* (2016) also observed increased GSH content in *gsnor1-3* compared to the WT, but using 3,3'-diaminobenzidine staining similar $H_2O_2$ levels were detected in *gsnor1-3* and the WT. It is also interesting that Zn did not modify GSH levels in the WT and *35S::FLAG-GSNOR1* plants, but significantly decreased the relatively high GSH content in *gsnor1-3*. Recently, the direct interaction between $H_2O_2$ and GSNOR has been revealed where the $H_2O_2$ inducer paraquat caused catalytic Zn release from GSNOR protein causing activity loss of the enzyme (Kovács *et al.*, 2016). Therefore, we examined the possibility whether Zn-induced $H_2O_2$ influences the activity of GSNOR in the WT and in *35S::FLAG-GSNOR1*. Exogenously applied GSH (1 mM) had no effect on control plants, but resulted in decreased $H_2O_2$ levels in case of Zn-treated plants (Fig 6C). Similarly, in Zn+GSH-treated plants significantly higher GSNOR activity was measured compared to plants treated with Zn alone (Fig 6D). The results indicate

that the reduction of Zn-induced $H_2O_2$ can ameliorate GSNOR activity loss suggesting that Zn-triggered $H_2O_2$ is directly involved in the inactivation of GSNOR possibly through catalytic $Zn^{2+}$ release as described by Kovács *et al.* (2016). This is further confirmed by the unaffected protein abundance in Zn-treated plants (Fig 3C and Fig S1). Moreover, a slight shift can be observed in the running of GSNOR protein in the gel (Fig 3C) suggesting that Zn induces alterations in protein structure which may be possible through $Zn^{2+}$ release.

**Zn induces distinct changes in protein nitration in *Arabidopsis* lines**

Nitric oxide reacts with superoxide anion to form peroxynitrite, the major RNS being involved in protein nitration processes (Sawa *et al.*, 2000). Treatment with Zn increased superoxide levels only in the roots of *35S::FLAG-GSNOR1*, in the other plant lines it remained unchanged (Fig 7A). Total SOD activity decreased in Zn-treated *35S::FLAG-GSNOR1* (Fig 7B) possibly contributing to superoxide level increase (Fig 7A). In *gsnor1-3*, a moderate increment in SOD activity was observed, while Zn-exposed WT plants showed unmodified SOD activities compared to the optimal Zn supply. The activities of MnSOD and FeSOD isoforms exceeded Cu/Zn SOD activities in the control plants (Fig 7C) but Zn modified this isoenzyme pattern since it reduced the activity of FeSOD and MnSOD and increased Cu/Zn SOD activity in all three *Arabidopsis* lines. The reduced availability of Mn and Fe as the effect of excess Zn (Ebbs and Kochian, 1997; Monnet *et al.*, 2001) can be the reason for the decreased MnSOD and FeSOD activities. The 250 μM concentration of applied Zn proved to be an appropriate concentration to increase the activity of Cu/Zn SOD as its cofactor (Feigl *et al.*, 2016). Protein nitration, as the marker of nitrosative stress, has previously been shown to be increased by the effect of Zn stress (300 μM) in *Brassica* species (Feigl *et al.*, 2015; 2016). In the present system, the protein bands showing immunopositivity towards 3-nitrotyrosine antibody have been detected in the low molecular weight range (16-30 KDa, Fig 7D). Here, eight protein bands were selected, and the intensities of the bands were evaluated by GelQuant (Fig S3). In general, most protein bands showed slight Zn-induced intensification in WT and in *35S::FLAG-GSNOR1*, while in the GSNOR deficient line, Zn reduced the nitration of most bands. The physiological nitroproteome of the observed *Arabidopsis* lines were similar in size and the applied Zn concentration did induce the appearance of newly nitrated protein bands in none of the *Arabidopsis* lines (Fig 7D). In the WT, the Zn-induced mild enhancement in protein nitration may be related to the moderate production of NO and superoxide (Fig 4A and Fig 7A). In *35S::FLAG-GSNOR1*, reduction in NO levels could be compensated by the superoxide formation resulting in slightly increased

nitration. In case of *gsnor1-3*, there were less nitrated proteins as the effect of Zn compared to control, which can be achieved by the activation of putative denitration processes (not yet known in plants, Kolbert *et al.*, 2017) or by enhanced degradation of nitrated proteins.

## Conclusion

Our data collectively indicate that Zn-induced $H_2O_2$ is directly involved in GSNOR inactivation and it positively regulates GSNO/SNO levels which in turn induces the S-nitrosation APX1 enzyme. The activity changes of APX and CAT may influence $H_2O_2$ levels in Zn-stressed plants (Fig 8). This means that Zn-induced $H_2O_2$ may influence its own level through a self-regulatory process which involves SNO signalling. These data provide novel evidence for the regulatory interplay between ROS ($H_2O_2$) and SNO signalling in *Arabidopsis* plants affected by metal stress.

**Supplementary material**

**Fig S1** Quantification of GSNOR protein amount (pixel density) in control and Zn-treated WT, *35S::FLAG-GSNOR1* and *gsnor1-3 Arabidopsis* seedlings using Gelquant software.

**Fig S2** Quantification of APX protein amount (pixel density) in control and Zn-treated WT, *35S::FLAG-GSNOR1* and *gsnor1-3 Arabidopsis* seedlings using Gelquant software. Detected bands are numbered.

**Fig S3** Quantification of nitrated protein amount (pixel density) in control and Zn-treated WT, *35S::FLAG-GSNOR1* and *gsnor1-3 Arabidopsis* seedlings using Gelquant software. Detected bands are numbered.

**Table S1** List of primers used in this study

**Table S2** *In vitro* S-nitrosation of proteins in *Arabidopsis* seedlings. Proteins were analysed by nanoLC-MS/MS after tryptic digestion. The MASCOT search engine was used to parse MS data to identify proteins from primary sequence databases. The acquired spectra were loaded into the Progenesis QI for proteomics software (version 4.0; Nonlinear Dynamics) for MS1 intensity based label-free quantification. Accession number: TAIR database accession number. Molecular mass in kDa. The ratio between +Asc and –Asc for each replicate is given.

**Table S3** *In vivo* S-nitrosation of proteins in *Arabidopsis* seedlings. Proteins were analysed by nanoLC-MS/MS after tryptic digestion. The MASCOT search engine was used to parse MS data to identify proteins from primary sequence databases. The acquired spectra were loaded into the Progenesis QI for proteomics software (version 4.0; Nonlinear Dynamics) for MS1 intensity based label-free quantification. Accession number: TAIR database accession number. Molecular mass in kDa. The ratio between +Asc and –Asc for each replicate is given.

**Table S4** Raw proteomics data

**Acknowledgements**

We thank for Éva Kapásné Török and for Elke Mattes for the excellent technical assistance. This work was supported by the János Bolyai Research Scholarship of the Hungarian Academy of Sciences (Grant no. BO/00751/16/8) by the National Research, Development and Innovation Fund (Grant no. NKFI-6, K120383 and PD120962) and by the EU-funded Hungarian grant EFOP-3.6.116-2016-00008. Zs. K. was supported by UNKP-18-4 New National Excellence Program of the Ministry of Human Capacities. Some of the experiments were carried out by Zs.K. during a 3-month-long visit at the Institute of Biochemical Plant Pathology, Helmholtz Zentrum München supported by TEMPUS

543 Foundation in the frame of the Hungarian Eötvös Scholarship (MAEÖ-1060-4/2017). This
544 work was also supported by the Bundesministerium für Bildung und Forschung.
545
546
547
548
549

**References**

**Arnér ESJ, Zhong L, Holmgren A.** 1999. Preparation and assay of mammalian thioredoxin and thioredoxin reductase. Methods in Enzymology **300,** 226-239.

**Bartha B, Kolbert Zs, Erdei L.** 2005. Nitric oxide production induced by heavy metals in *Brassica juncea* L. Czern. and *Pisum sativum* L. Acta Biologica Szegediensis **49,** 9–12.

**Beauchamp C, Fridovich I.** 1971. Superoxide dismutase: improved assays and an assay applicable to acrylamide gels. Analytical Biochemistry **44,** 276–287.

**Begara-Morales JC, Sánchez-Calvo B, Chaki M, Valderrama R, Mata-Pérez C, López-Jaramillo J, Padilla MN, Carreras A, Corpas, FJ, Barroso JB.** 2014. Dual regulation of cytosolic ascorbate peroxidase (APX) by tyrosine nitration and S-nitrosylation. Journal of Experimental Botany **65,** 527–538.

**Blum H, Beier H, Gross HJ.** 1987. Improved silver staining of plant proteins, RNA and DNA in polyacrylamide gels. Electrophoresis **8,** 93-99.

**Bradford MM.** 1976. A rapid and sensitive method for the quantitation of microgram quantities of protein utilizing the principle of protein-dye binding. Analytical Biochemistry **72,** 248–254.

**Chaki M, Valderrama R, Fernández-Ocaña AM. et al.** 2011. Mechanical wounding induces a nitrosative stress by down-regulation of GSNO reductase and an increase in S-nitrosothiols in sunflower (*Helianthus annuus*) seedlings. Journal of Experimental Botany **62,** 1803-1813.

**Chaki M, Álvarez de Morales P, Ruiz C, Begara-Morales JC, Barroso JB, Corpas FJ, Palma JM.** 2015. Ripening of pepper (*Capsicum annuum*) fruit is characterized by an enhancement of protein tyrosine nitration. Annals of Botany **116,** 637-647.

**Chen R, Sun S, Wang C, Li Y, Liang Y, An F, Li C, Dong H, Yang X, Zhang J, Zuo J.** 2009. The Arabidopsis PARAQUAT RESISTANT2 gene encodes an S-nitrosoglutathione reductase that is a key regulator of cell death. Cell Research **19,** 1377–1387.

**Corpas FJ, Palma JM, del Río LA, Barroso JB.** 2013. Protein tyrosine nitration in higher plants grown under natural and stress conditions. Frontiers in Plant Science **4,** 29. doi: 10.3389/fpls.2013.00029

**Cuypers A, Vangronsveld J, Clijsters H.** 2002. Peroxidases in roots and primary leaves of *Phaseolus vulgaris* copper and zinc phytotoxicity: a comparison. Journal of Plant Physiology **159,** 869–876.

**Dhindsa RS, Plumb-Dhindsa P, Thorpe TA.** 1981. Leaf senescence: correlated with increased levels of membrane permeability and lipid peroxidation, and decreased levels of superoxide dismutase and catalase. Journal of Experimental Botany **32,** 93–101.

**Di Baccio D, Kopriva S, Sebastiani L, Rennenberg H.** 2005. Does glutathione metabolism have a role in the defence of poplar against zinc excess? New Phytologist **167,** 73–80.

**Ebbs SD, Kochian LV.** 1997. Toxicity of zinc and copper to *Brassica* species: implications for phytoremediation. Journal of Environmental Quality **26,** 776-781.

**Feechan A, Kwon E, Yun BW, Wang Y, Pallas JA, Loake GJ.** 2005. A central role for S-nitrosothiols in plant disease resistance. Proceedings of the National Academy of Sciences of the United States of America **102,** 8054-8059.

**Feigl G, Lehotai N, Molnár Á, Ördög A, Rodríguez-Ruiz M, Palma JM, Corpas FJ, Erdei L, Kolbert Zs.** 2015. Zinc induces distinct changes in the metabolism of reactive oxygen and nitrogen species (ROS and RNS) in the roots of two Brassica species with different sensitivity to zinc stress. Annals of Botany **116,** 613-625.

**Feigl G, Kolbert Zs, Lehotai N, Molnár Á, Ördög A, Bordé Á, Laskay G, Erdei L.** 2016. Different zinc sensitivity of Brassica organs is accompanied by distinct responses in protein nitration level and pattern. Ecotoxicology and Environmental Safety **125,** 141-152.

**Frungillo L, Skelly MJ, Loake GJ, Spoel SH, Salgado I.** 2014. S-nitrosothiols regulate nitric oxide production and storage in plants through the nitrogen assimilation pathway. Nature Communications **5,** 5401 doi: 10.1038/ncomms6401

**Galetskiy D, Lohscheider JN, Kononikhin AS, Popov IA, Nikolaev EN, Adamska I.** 2011. Phosphorylation and nitration levels of photosynthetic proteins are conversely regulated by light stress. Plant Molecular Biology **77,** 461–473.

**Gallé Á, Csiszár J, Secenji M, Guóth A, Cseuz L, Tari I, Györgyey J, Erdei L.** 2009. Glutathione transferase activity and expression patterns during grain filling in flag leaves of wheat genotypes differing in drought tolerance: response to water deficit. Journal of Plant Physiology **166,** 1878-1891.

**Gow AJ, Farkouh CR, Munson DA, Posencheg MA, Ischiropoulos H.** 2004. Biological significance of nitric oxide-mediated protein modifications. American Journal of Physiology-Lung Cellular and Molecular Physiology **287,** L262–L268.

**Gupta B, Pathak GC, Pandey N.** 2011. Induction of oxidative stress and antioxidant responses in *Vigna mungo* by zinc stress. Russian Journal of Plant Physiology **58,** 85–91.

**Helmersson A, von Arnold S, Bozhkov PV.** 2008. The level of free intracellular zinc mediates programmed cell death/cell survival decisions in plant embryos. Plant Physiology **147,** 1158–1167.

**Holzmeister C, Fröhlich A, Sarioglu H, Bauer N, Durner J, Lindermayr C.** 2011. Proteomic analysis of defense response of wildtype *Arabidopsis thaliana* and plants with impaired NO- homeostasis. Proteomics **11,** 1664–1683.

**Jain P, Bhatla SC.** 2017. Molecular mechanisms accompanying nitric oxide signalling through tyrosine nitration and S-nitrosylation of proteins in plants. Functional Plant Biology **45,** 70-82.

**Jain R, Srivastava S, Solomon S, Shrivastava AK, Chandra A.** 2010. Impact of excess zinc on growth parameters, cell division, nutrient accumulation, photosynthetic pigments and oxidative stress of sugarcane (Saccharum spp.). Acta Physiologiae Plantarum **32,** 979–986.

**Kato M, Shimizu S.** 1987. Chlorophyll metabolism in higher plants. VII. Chlorophyll degradation in senescing tobacco leaves; phenolic-dependent peroxidative degradation Canadian Journal of Botany **65,** 729–735.

**Kiekens L.** 1995. Zinc. In: Alloway BJ, ed. Heavy Metals in Soils. London: Blackie Academic and Professional, 284-305.

**Kneeshaw S, Gelineau S, Tada Y, Loake GJ, Spoel SH.** 2014. Selective protein denitrosylation activity of thioredoxin-h5 modulates plant immunity. Molecular Cell **56,** 153-162.

**Kolbert Zs, Pető A, Lehotai N, Feigl G, Ördög A, Erdei L**. 2012. *In vivo* and *in vitro* studies on fluorophore-specificity. Acta Biologica Szegediensis **56,** 37–41.

**Kolbert Zs, Feigl G, Bordé Á, Molnár Á, Erdei L.** 2017. Protein tyrosine nitration in plants: Present knowledge, computational prediction and future perspectives. Plant Physiology and Biochemistry **113,** 56-63.

**Kovacs I, Holzmeister C, Wirtz M. et al.** 2016. ROS-mediated inhibition of S-nitrosoglutathione reductase contributes to the activation of anti-oxidative mechanisms. Frontiers in Plant Science **7,** 1669 doi: 10.3389/fpls.2016.01669

**Kwon E, Feechan A, Yun BW, Hwang BH, Pallas JA, Kang JG, Loake GJ.** 2012. AtGSNOR1 function is required for multiple developmental programs in *Arabidopsis*. Planta **236,** 887–900.

**Lamotte O, Bertoldo JB, Besson-Bard A, Rosnoblet C, Aimé S, Hichami S, Terenzi H, Wendehenne D.** 2014. Protein S-nitrosylation: specificity and identification strategies in plants. Frontiers in Chemistry **2,** 114. doi: 10.3389/fchem.2014.00114

**Lee U, Wie C, Fernandez BO, Feelisch M, Vierling E.** 2008. Modulation of nitrosative stress by S-nitrosoglutathione reductase is critical for thermotolerance and plant growth in *Arabidopsis*. Plant Cell **20,** 786–802.

**Lehotai N, Kolbert Zs, Pető A, Feigl G, Ördög A, Kumar D, Tari I, Erdei L.** 2012. Selenite-induced hormonal and signalling mechanisms during root growth of *Arabidopsis thaliana* L. Journal of Experimental Botany **63,** 5677-5687.

**Li X, Yang Y, Jia L, Chen H, Wei X.** 2013. Zinc-induced oxidative damage, antioxidant enzyme response and proline metabolism in roots and leaves of wheat plants. Ecotoxicology and Environmental Safety **89,** 150–157.

**Lindermayr, C.** 2018. Crosstalk between reactive oxygen species and nitric oxide in plants: Key role of S-nitrosoglutathione reductase. Free Radical Biology and Medicine **122,** 110-115.

**Lucini L, Bernardo L.** 2015. Comparison of proteome response to saline and zinc stress in lettuce. Frontiers in Plant Science **6,** 240 doi: 10.3389/fpls.2015.00240

**Monnet F, Vaillant N, Vernay P, Coudret A, Sallanon H, Hitmi A. 2001.** Relationship between PSII activity, $CO_2$ fixation, and Zn, Mn and Mg contents of *Lolium perenne* under zinc stress. Journal of Plant Physiology **158,** 1137-1144.

**Morina F, Jovanovic L, Mojovic M, Vidovic M, Pankovic D, Veljovic Jovanovic S**. 2010. Zinc-induced oxidative stress in Verbascum thapsus is caused by an accumulation of reactive oxygen species and quinhydrone in the cell wall. Physiologia Plantarum **140,** 209-224.

**Nakano Y, Asada K.** 1981. Hydrogen peroxide is scavenged by ascorbate specific peroxidase in spinach chloroplasts. Plant and Cell Physiology **22,** 867–880.

**Noulas C, Tziouvalekas M, Karyotis T.** 2018. Zinc in soils, water and food crops. Journal of Trace Elements in Medicine and Biology **49,** 252-260.

**Papdi C, Ábrahám E, Joseph MP, Popescu C, Koncz C, Szabados L.** 2008. Functional identification of *Arabidopsis* stress regulatory genes using the controlled cDNA overexpression system. Plant Physiology **147,** 528-542.

**Pető A, Lehotai N, Feigl G, Tugyi N, Ördög A, Gémes K, Tari I, Erdei L, Kolbert Z.** 2013. Nitric oxide contributes to copper tolerance by influencing ROS metabolism in *Arabidopsis.* Plant Cell Reports **32,** 1913-1923.

**Prats E, Carver TLW, Mur LAJ.** 2008. Pathogen-derived nitric oxide influences formation of the appressorium infection structure in the phytopathogenic fungus *Blumeria graminis*. Research in Microbiology **159,** 476-480.

**Ramakrishna B, Rao SS.** 2015. Foliar application of brassinosteroids alleviates adverse effects of zinc toxicity in radish (*Raphanus sativus* L.) plants. Protoplasma **252,** 665-677.

**Sagardoy R, Morales F, López□Millán AF, Abadía A, Abadía J.** 2009. Effects of zinc toxicity on sugar beet (*Beta vulgaris* L.) plants grown in hydroponic. Plant Biology **11,** 339-350.

**Sakamoto A, Ueda M, Morikawa H.** 2002. *Arabidopsis* glutathione-dependent formaldehyde dehydrogenase is an S-nitrosoglutathione reductase. FEBS Letters **515,** 20–24.

**Sawa T, Akaike T, Maeda H.** 2000. Tyrosine nitration by peroxynitrite formed from nitric oxide and superoxide generated by xanthine oxidase. The Journal of Biological Chemistry **275,** 32467-32474.

**Sharma SK, Goloubinoff P, Christen P.** 2008. Heavy metal ions are potent inhibitors of protein folding. Biochemical and Biophysical Research Communications **372,** 341–345.

**Tari I, Csiszár J, Horváth E, Poór P, Takács Z, Szepesi Á.** 2015. Alleviation of the adverse effect of salt stress in tomato by salicylic acid shows time- and organ-specific antioxidant response. Acta biologica Cracoviensia. *Series botanica* **57,** 21-30.

**Tewari RK, Kumar P, Sharma PD.** 2008. Morphology and physiology of zinc stressed mulberry plants. Journal of Plant Nutrition and Soil Science **171,** 286–294.

**Thompson JW, Forrester MT, Moseley MA, Foster MW.** 2013. Solid-phase capture for the detection and relative quantification of S-nitrosoproteins by mass spectrometry. Methods **62,** 130–137.

**Ticha T, Cincalova L, Kopecny D. Sedlářová M, Kopečná M, Luhová L, Petřivalský M** 2017. Characterization of S-nitrosoglutatione reductase from *Brassica* and *Lactuca* ssp. and its modulation during plant development. Nitric Oxide **68,** 68-76.

**Umbreen A, Lubega J, Cui B, Pan Q, Jiang J, Loake GJ.** 2018. Specificity of nitric oxide signalling. Journal of Experimental Botany **19,** 3439-3448.

**van der Vliet A, Eiserich JP, Shigenana MK, Cross CE.** 1999. Reactive nitrogen species and tyrosine nitration in the respiratory tract: epiphenomena or a pathobiologic mechanism of disease? American Journal of Respiratory and Critical Care Medicine **160,** 1–9.

**Weckx JEJ, Clijsters HMM.** 1997. Zn phytotoxicity induces oxidative stress in primary leaves of Phaseolus vulgaris. Plant Physiology and Biochemistry **35,** 405-410.

**Welinder C, Ekblad L.** 2011. Coomassie staining as loading control in Western blot analysis. Journal of Proteome Research **10,** 1416-1419.

**Wiśniewski JR, Zougman A, Nagaraj N, Mann M.** 2009. Universal sample preparation method for proteome analysis. Nature Methods **6,** 359-362.

**Xu J, Yin H, Li Y, Liu X.** 2010. Nitric oxide is associated with long-term zinc tolerance in *Solanum nigrum.* **154,** 1319–1334.

**Yang H, Mu J, Chen L, Feng J, Hu J, Li L, Zhou JM, Zuo J.** 2015. S-nitrosylation positively regulates ascorbate peroxidase activity during plant stress responses. Plant Physiology **167,** 1604-1615.

**Zaffagnini M, De Mia M, Morisse S, Di Giacinto N, Marchand CH, Maes A, Lemaire SD, Trost P.** 2015. Protein S-nitrosation in photosynthetic organisms: A comprehensive overview with future perspectives. Biochimica et Biophysica Acta (BBA) - Proteins and Proteomics **1864,** 952-966.

**Zarcinas BA, Ishak CF, McLaughlin MJ, Cozens G. 2004.** Heavy metals in soils and crops in Southeast Asia. Environmental Geochemistry and Health **26,** 343–357.

**Figure legends**

**Fig 1 Zinc tolerance of *Arabidopsis* seedlings**. (A) Average seedling fresh weight of 7-days-old WT, *35S::FLAG-GSNOR1* and *gsnor1-3* plants grown without (control, 15 µM) or with 250 µM Zn. (B) Zn tolerance indexes (% of control) of 250 µM Zn-treated *Arabidopsis* lines. Different letters indicate significant differences according to Duncan's test (n=20, P≤0.05). (C) Representative images showing 7-days-old control and 250 µM Zn-treated WT, *35S::FLAG-GSNOR1* and *gsnor1-3 Arabidopsis*. Bar=1 cm.

**Fig 2 Zinc accumulation of *Arabidopsis* seedlings.** Zn levels (estimated by Zinquin staining) in the differentiation zone (A) and meristematic region (B) of primary roots in case of control and 250 µM Zn-treated *WT, 35S::FLAG-GSNOR1* and *gsnor1-3* plants. Different letters indicate significant differences according to Duncan's test (n=10, P≤0.05). (D) Representative images showing Zinquin-stained segments of the primary roots (differentiation zone, C and root tips, D). Bars=500 µm.

**Fig 3 Zinc affects GSNOR activity, protein and transcript level in *Arabidopsis* seedlings**. Activity (A) of GSNOR enzyme and relative transcript level (B) of *GSNOR1* gene in control and Zn-treated *WT, 35S::FLAG-GSNOR1* and *gsnor1*-3 seedlings. Data of transcript levels were normalised using the *A. thaliana ACTIN2* and *GAPDH2* genes as internal controls. The relative transcript level in control samples was arbitrarily considered to be 1. Different letters indicate significant differences according to Duncan's test (n=5, P≤0.05). (C) GSNOR protein abundance in *WT, 35S::FLAG-GSNOR1* and *gsnor1-3* seedlings grown under control conditions or in the presence of 250 µM Zn. Input controls were visualized by Coomassie staining. Band intensities were measured using GelQuant software and the data are presented as Fig S1.

**Fig 4 NO and SNO levels are differentially affected by zinc in *Arabidopsis* GSNOR mutants.** Nitric oxide levels (A) in the root tips and SNO levels (B) in whole seedlings of *WT, 35S::FLAG-GSNOR1* and *gsnor1-3* treated with Zn or grown under control conditions. (C) NADPH-dependent thioredoxin reductase (NTR) activity in control and Zn-treated *Arabidopsis* seedlings. (D) Relative transcript levels of *TRXh3* gene in *WT, 35S::FLAG-GSNOR1* and *gsnor1-3* grown in the presence or absence (control) of excess Zn. Data of transcript levels were normalised using the *A. thaliana ACTIN2* and *GAPDH2* genes as internal controls. The relative transcript level in control samples was arbitrarily considered to be 1. Different letters indicate significant differences according to Duncan's test (n=10, 5-7 or 5, respectively, P≤0.05).

**Fig 5 Zinc induced protein S-nitrosation examined by RSNO-RAC.** (A) Silver-stained SDS gel (12%) showing S-nitrosation in control and Zn-treated wild-type *Arabidopsis* seedlings. S-nitrosylated proteins were extracted by RSNO-RAC method. Sample homogenates treated with 1 mM GSNO served as positive control while those to which ascorbate was not added served as negative controls. Input controls were visualized by Coomassie staining. B) Zn-induced S-nitrosation of proteins in *Arabidopsis* seedlings. Proteins were analysed by nanoLC-MS/MS after tryptic digestion. The MASCOT search engine was used to parse MS data to identify proteins from primary sequence databases. The acquired spectra were loaded into the Progenesis QI for proteomics software (version 4.0; Nonlinear Dynamics) for MS1 intensity based label-free quantification. Accession number: TAIR database accession number. Molecular mass in kDa. The ratio between +Asc and –Asc for each replicate is given. Total activity of APX (C) and catalase (D) in control and Zn-treated *WT, 35S::FLAG.GSNOR1* and *gsnor1-3* seedlings. Different letters indicate significant differences according to Duncan's test (n= 5, $P \leq 0.05$). (E) APX protein amount in control and Zn-treated WT, *35S::FLAG-GSNOR1* and *gsnor1-3* seedlings. Pixel densities were measured using GelQuant software and the data are presented as Fig S2.

**Fig 6 Zinc-induced $H_2O_2$ accumulation and GSNOR activity loss can be reversed by exogenous GSH.** Hydrogen peroxide levels in the root system (A) and glutathione content (B) of *WT, 35S::FLAG-GSNOR1* and *gsnor1-3 Arabidopsis* grown in the presence or absence (control) of excess Zn. Hydrogen peroxide levels (C) and GSNOR activity (D) in *WT, 35S::FLAG-GSNOR1* and *gsnor1-3 Arabidopsis* treated with 0 or 250 µM Zn in the presence or absence of 1 mM GSH. Different letters indicate significant differences according to Duncan's test (n= 10 or 5, respectively $P \leq 0.05$).

**Fig 7 Zinc slightly affects superoxide metabolism and protein tyrosine nitration.** Superoxide anion level in the root (A) and total SOD activity (B) in of *WT, 35S::FLAG-GSNOR1* and *gsnor1-3 Arabidopsis* grown in the presence or absence (control) of Zn. (C) Native PAGE separation (10%) of SOD isoenzymes in control and Zn-treated *Arabidopsis* lines. (D) Western blot probed with rabbit anti-nitrotyrosine polyclonal antibody (1:2000). Commercial nitrated BSA was used as a positive control. The intensities of numbered bands were quantified by Gelquant software and the data are presented as Fig S3.

**Fig 8 Schematic model summarizing the data obtained in this study (solid lines) completed with literature data (dashed line).** The applied moderate Zn concentration induced mild superoxide and NO formation which may react with each other to form peroxynitrite. In turn, peroxynitrite induces slightly increased protein nitration. Zn resulted in

glutathione content decrease which may contribute to $H_2O_2$ formation. Zinc-induced $H_2O_2$ is directly involved in GSNOR inactivation which leads to SNO accumulation and intensified S-nitrosation. We identified APX1 as a target for S-nitrosation. According to the literature (Begara-Morales *et al.,* 2014, Yang *et al.,* 2015) this modification results in increased APX activity which would negatively influence $H_2O_2$ levels (indicated by dashed line). In our experimental system; however, the total activities of APX and also CAT decreased as the effect of Zn which may contribute to the $H_2O_2$ increase (solid lines). The activity loss of APX and CAT enzymes may be due to intensified protein nitration.

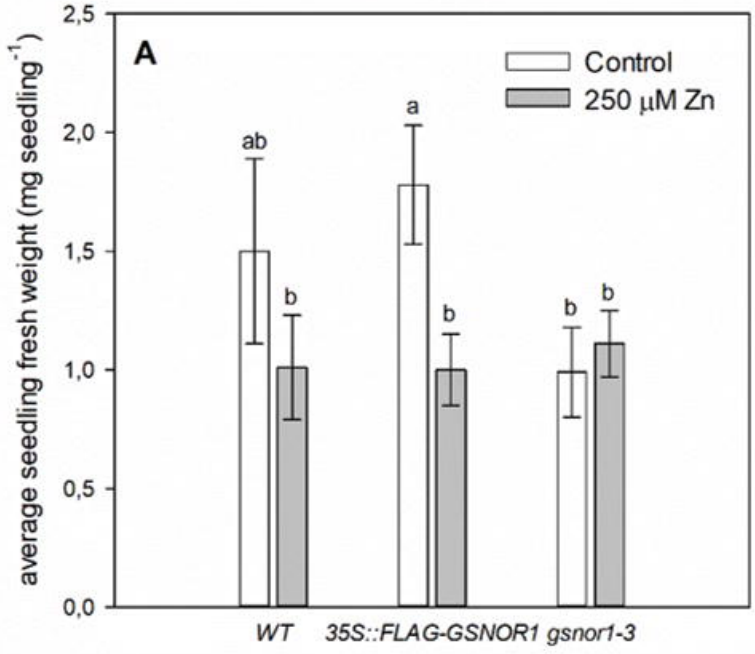
A
Control
250 µM Zn
average seedling fresh weight (mg seedling$^{-1}$)
2,5
2,0
1,5
1,0
0,5
0,0
ab
b
a
b
b
b
WT
35S::FLAG-GSNOR1
gsnor1-3

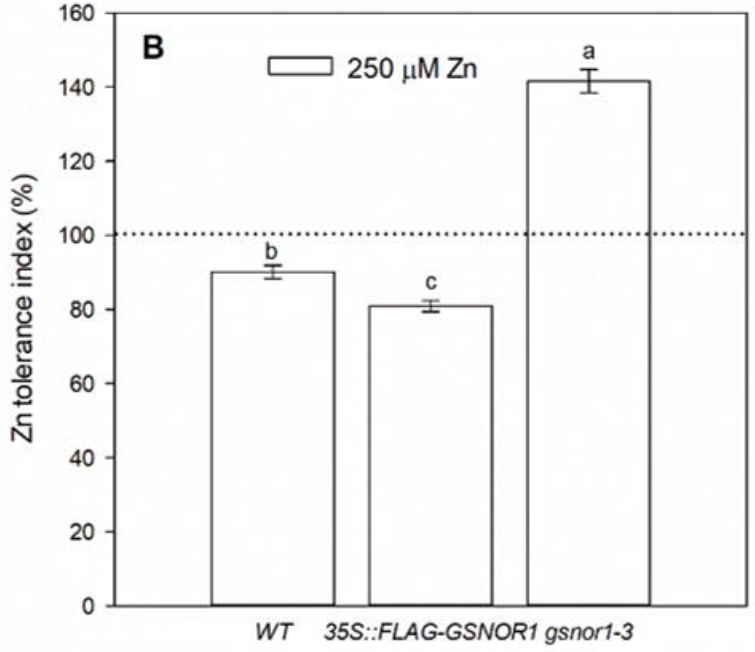
B
250 µM Zn
Zn tolerance index (%)
160
140
120
100
80
60
40
20
0
b
c
a
WT
35S::FLAG-GSNOR1
gsnor1-3

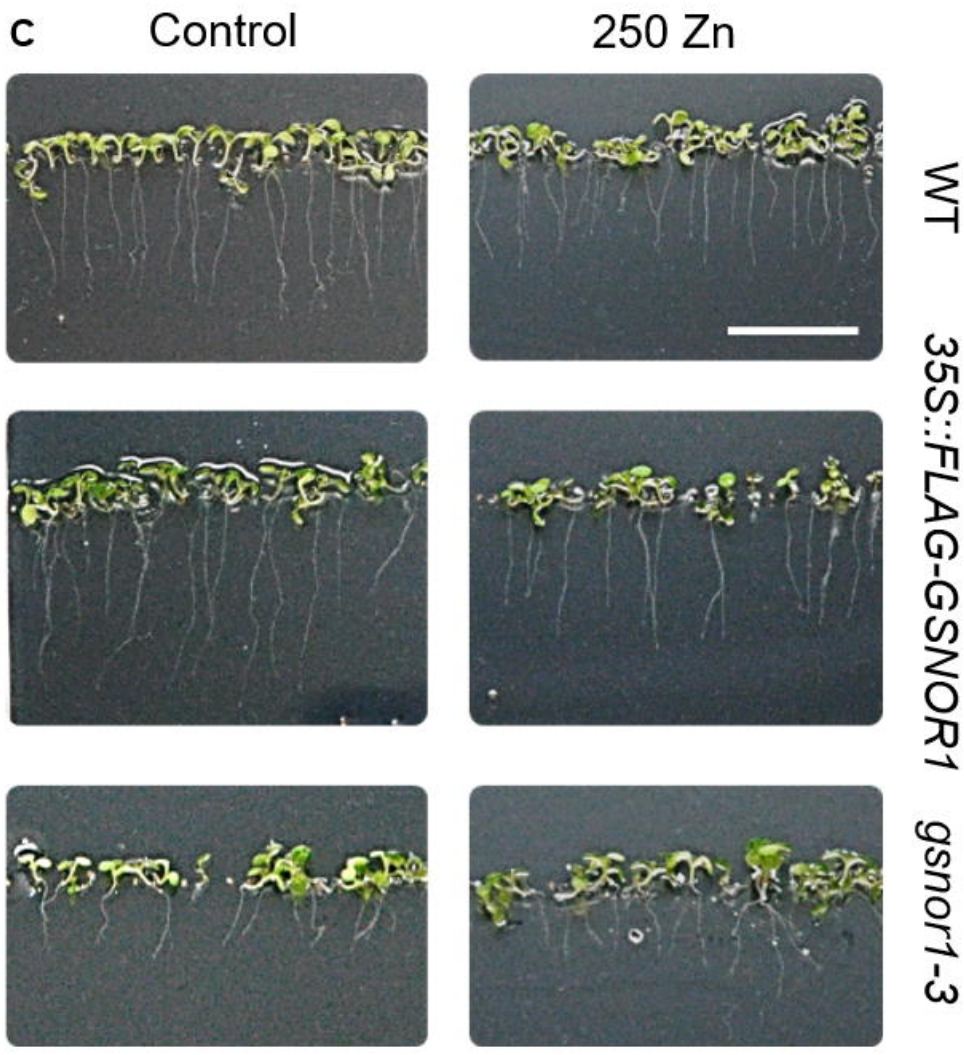
C
Control
250 Zn
WT
35S::FLAG-GSNOR1
gsnor1-3

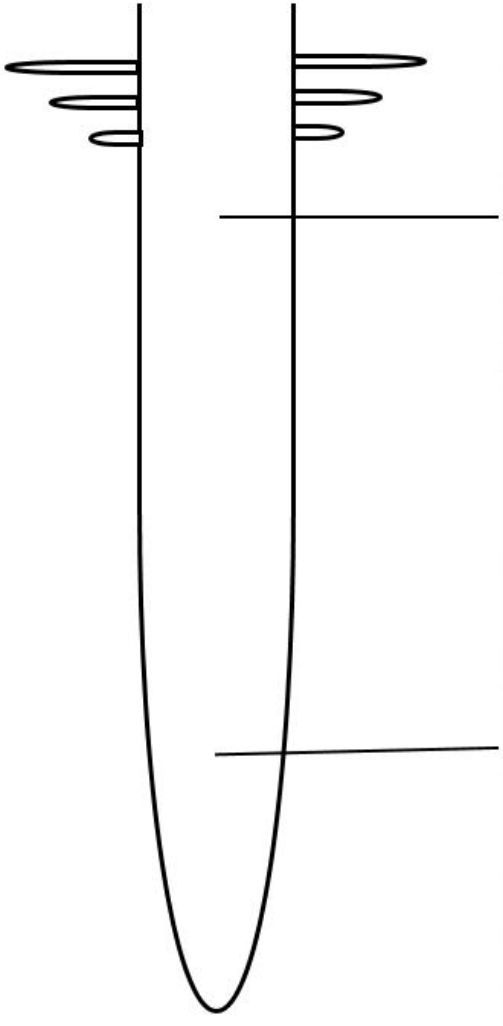

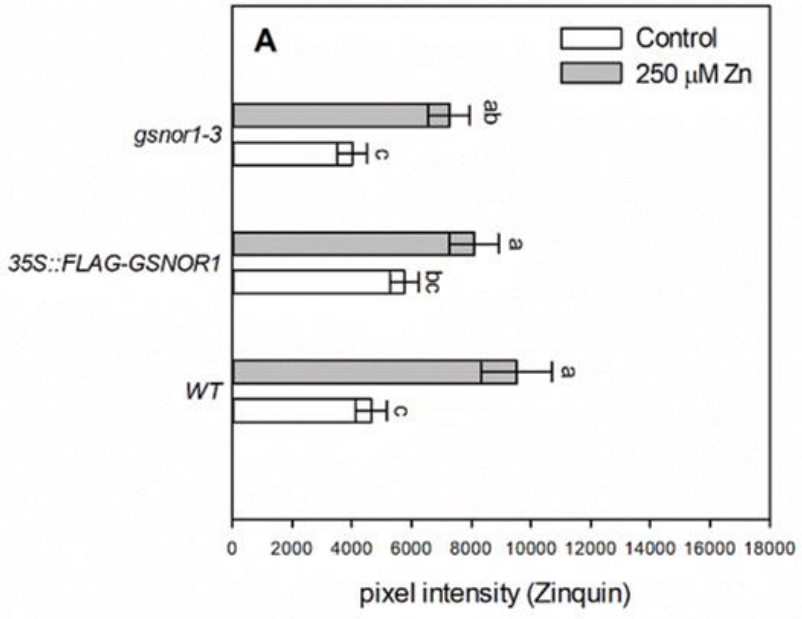
A
Control
250 μM Zn
gsnor1-3
35S::FLAG-GSNOR1
WT
ab
c
a
bc
a
c
0 2000 4000 6000 8000 10000 12000 14000 16000 18000
pixel intensity (Zinquin)

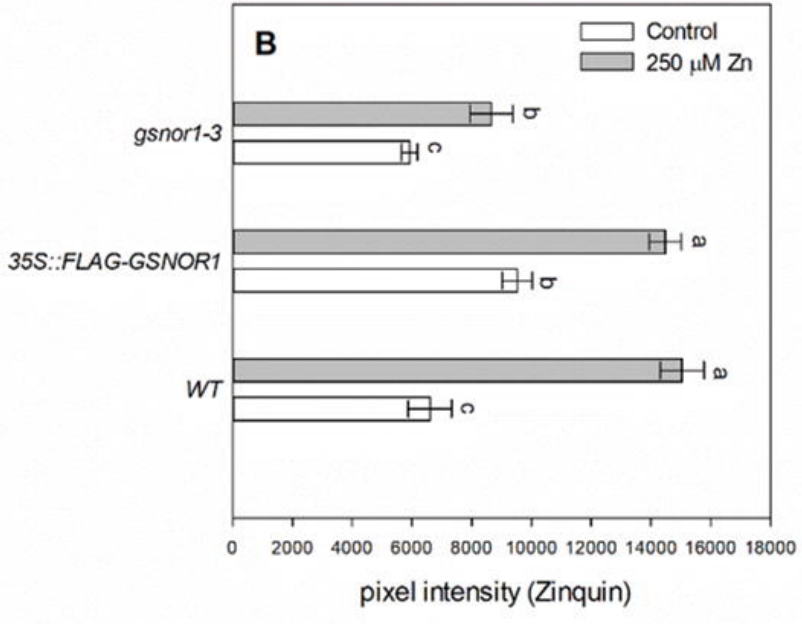
B
Control
250 μM Zn
gsnor1-3
35S::FLAG-GSNOR1
WT
b
c
a
b
a
c
0 2000 4000 6000 8000 10000 12000 14000 16000 18000
pixel intensity (Zinquin)

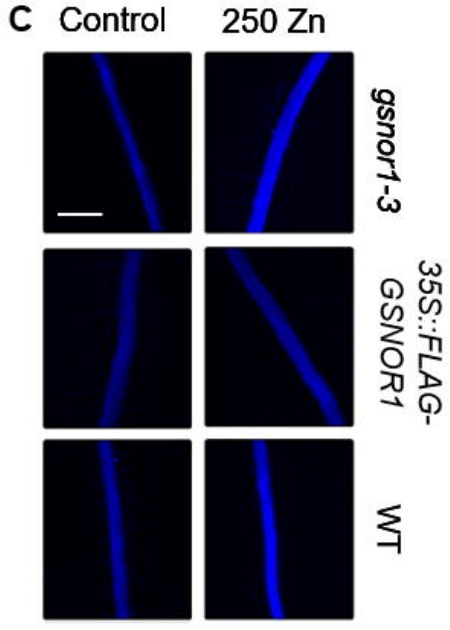
C
Control
250 Zn
gsnor1-3
35S::FLAG-GSNOR1
WT

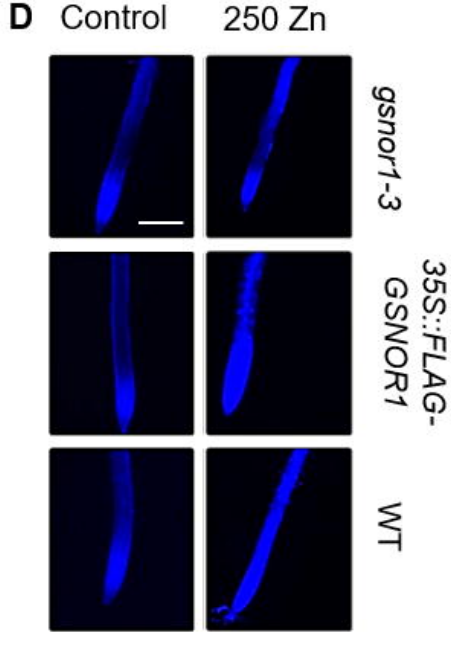
D
Control
250 Zn
gsnor1-3
35S::FLAG-GSNOR1
WT

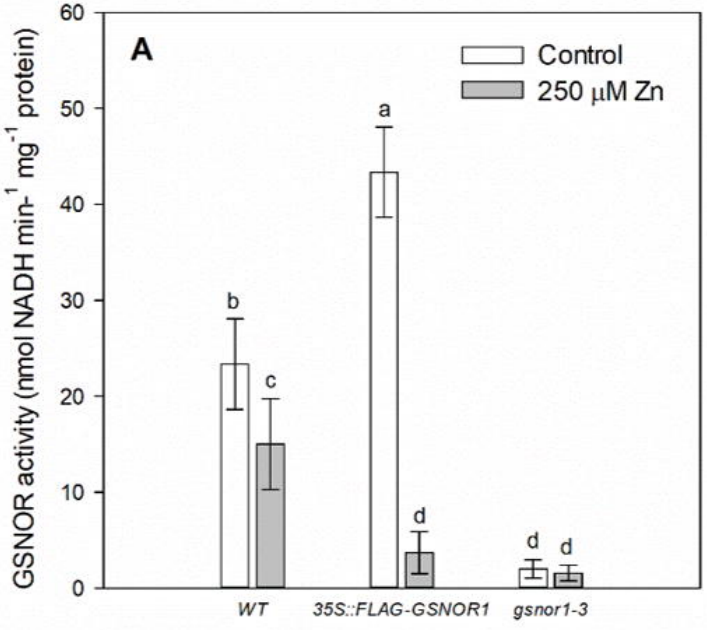
A
Control
250 μM Zn
GSNOR activity (nmol NADH min-1 mg-1 protein)
60
50
40
30
20
10
0
a
b
c
d
d
d
WT
35S::FLAG-GSNOR1
gsnor1-3

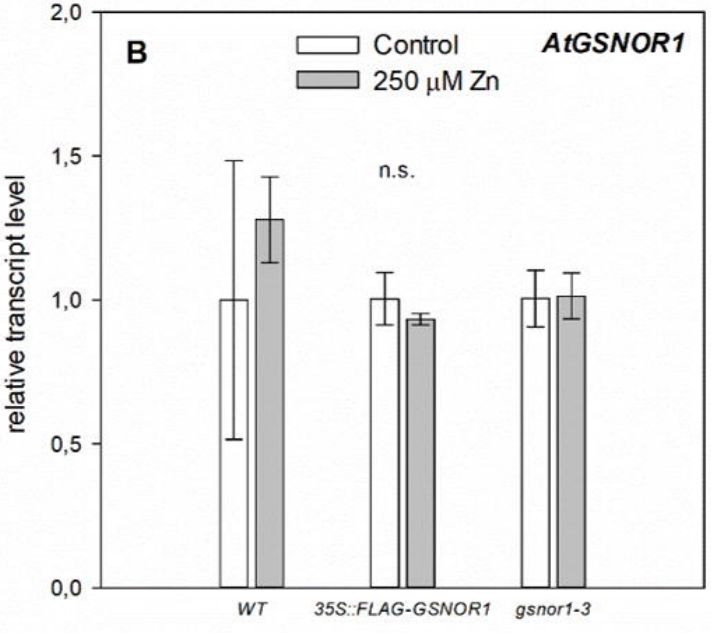
B
Control
250 μM Zn
AtGSNOR1
relative transcript level
2,0
1,5
1,0
0,5
0,0
n.s.
WT
35S::FLAG-GSNOR1
gsnor1-3

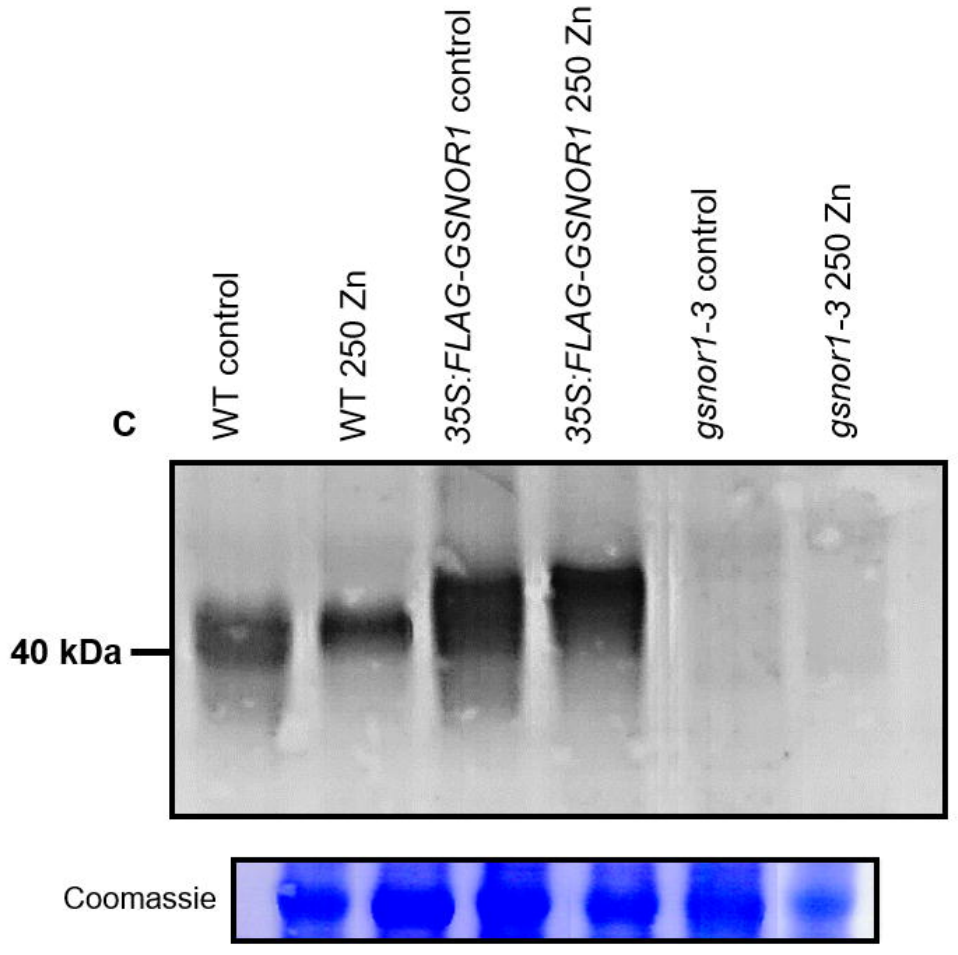
C
WT control
WT 250 Zn
35S:FLAG-GSNOR1 control
35S:FLAG-GSNOR1 250 Zn
gsnor1-3 control
gsnor1-3 250 Zn
40 kDa
Coomassie

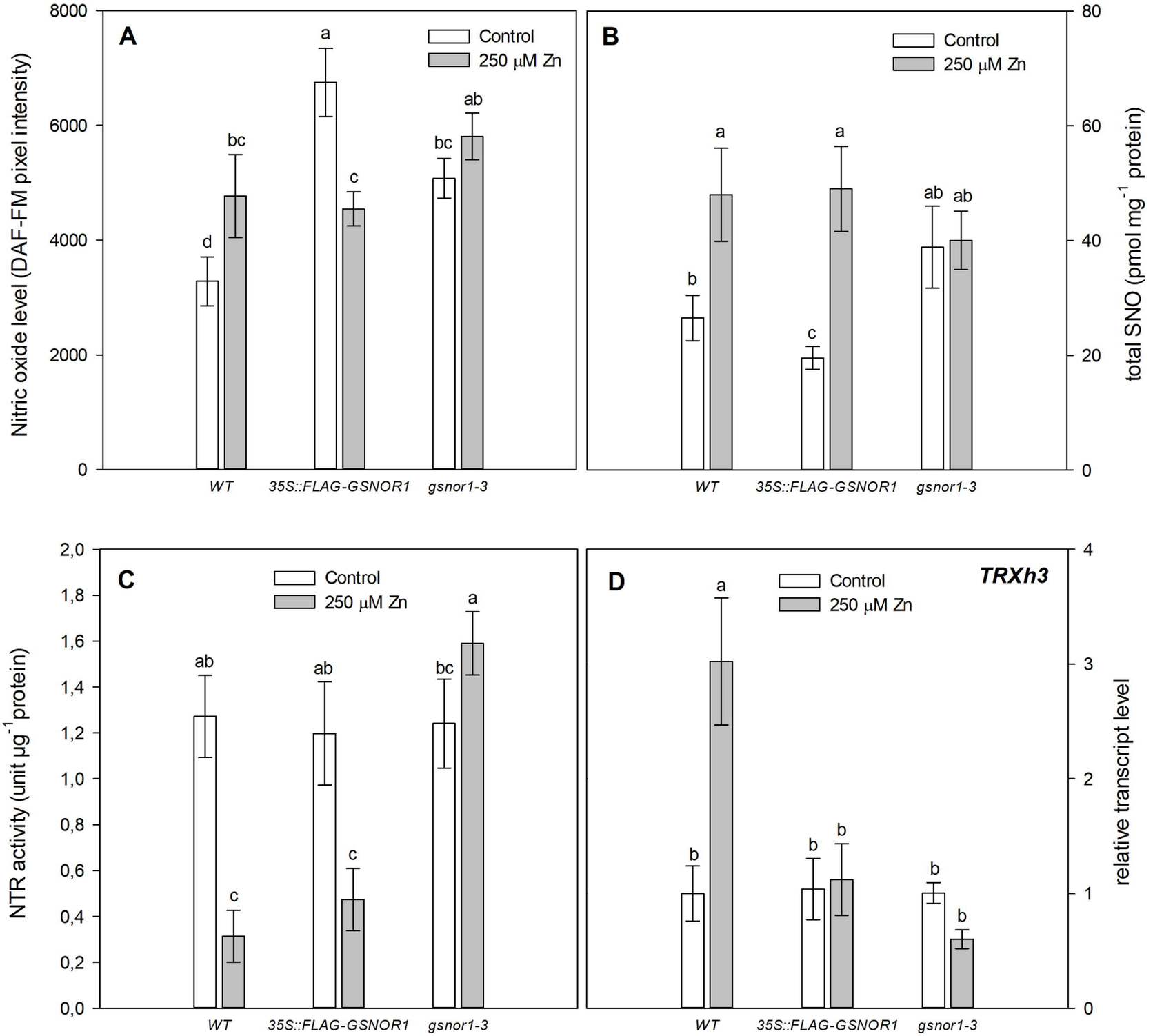
A
Control
250 μM Zn
Nitric oxide level (DAF-FM pixel intensity)
8000
6000
4000
2000
0
d
bc
a
c
bc
ab
WT
35S::FLAG-GSNOR1
gsnor1-3
B
Control
250 μM Zn
total SNO (pmol mg-1 protein)
80
60
40
20
0
b
a
c
a
ab
ab
WT
35S::FLAG-GSNOR1
gsnor1-3
C
Control
250 μM Zn
NTR activity (unit μg-1 protein)
2,0
1,8
1,6
1,4
1,2
1,0
0,8
0,6
0,4
0,2
0,0
ab
c
ab
c
bc
a
WT
35S::FLAG-GSNOR1
gsnor1-3
D
TRXh3
Control
250 μM Zn
relative transcript level
4
3
2
1
0
b
a
b
b
b
b
WT
35S::FLAG-GSNOR1
gsnor1-3

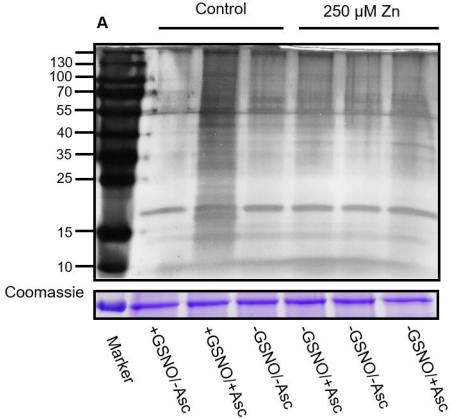


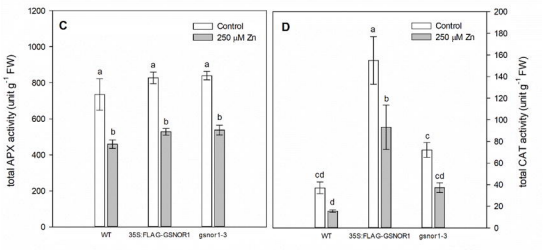


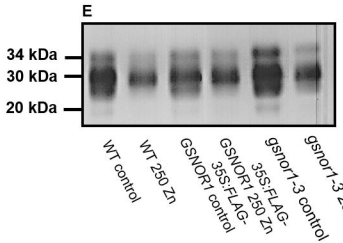


B

| Protein | kDa | Accession number | number of unique peptides | Ratio +Asc/-Asc repl. 1 | Ratio +Asc/-Asc repl. 2 | Ratio +Asc/-Asc repl. 3 |
|---|---|---|---|---|---|---|
| Lactate/malate dehydrogenase family protein | 35 | AT1G04410.1 | 2 | 10.12 | 66.35 | 5.71 |
| L-ascorbate peroxidase 1, cytosolic | 27 | AT1G07890.1 | 3 | 76.55 | 67.63 | 2.66 |
| Glyceraldehyde-3-phosphate dehydrogenase GAPC2, cytosolic | 37 | AT1G13440.1 | 5 | 7.25 | 6.87 | 2.27 |
| Ribosomal protein S5/Elongation factor G/III/V family protein | 94 | AT1G56070.1 | 7 | 4.15 | 3.29 | 2.94 |
| Glyceraldehyde-3-phosphate dehydrogenase GAPB, chloroplastic | 48 | AT1G42970.1 | 2 | 794.06 | 17.49 | 1.21 |
| Ribosomal protein L14p/L23e family protein | 15 | AT1G04480.1 | 2 | 7.96 | 4.33 | 1.80 |
| Ribosomal protein L19e family protein | 25 | AT1G02780.1 | 2 | 2.01 | 8.92 | 2.10 |
| photosynthetic electron transfer B | 24 | ATCG00720.1 | 5 | 2.11 | 5.97 | 1.73 |
| Ribosomal protein L22p/L17e family protein | 20 | AT1G27400.1 | 3 | 5.20 | 8.03 | 1.52 |
| Methionine adenosyltransferase 3 | 42 | AT2G36880.1 | 3 | 5.11 | 3.78 | 1.72 |
| Ribosomal protein 1 | 45 | AT1G43170.1 | 8 | 1.39 | 7.30 | 1.53 |
| ribulose bisphosphate carboxylase small chain 1A | 20 | AT1G67090.1 | 4 | 6.60 | 2.73 | 1.94 |
| Ribosomal protein S5 domain 2-like superfamily protein | 17 | AT5G18380.1 | 2 | 2.35 | 5.14 | 1.38 |
| Ribosomal protein S13/S15 | 17 | AT4G16720.1 | 2 | 1.59 | 11.04 | 1.12 |
| Cobalamin-independent synthase family protein | 84 | AT5G17920.1 | 8 | 3.24 | 2.93 | 1.44 |
| Enolase | 48 | AT2G36530.1 | 9 | 1.43 | 3.42 | 1.40 |
| tubulin alpha-4 chain | 50 | AT1G04820.1 | 4 | 1.30 | 2.19 | 1.70 |
| ribosomal protein 5B | 23 | AT2G37270.1 | 2 | 1.32 | 2.45 | 1.38 |

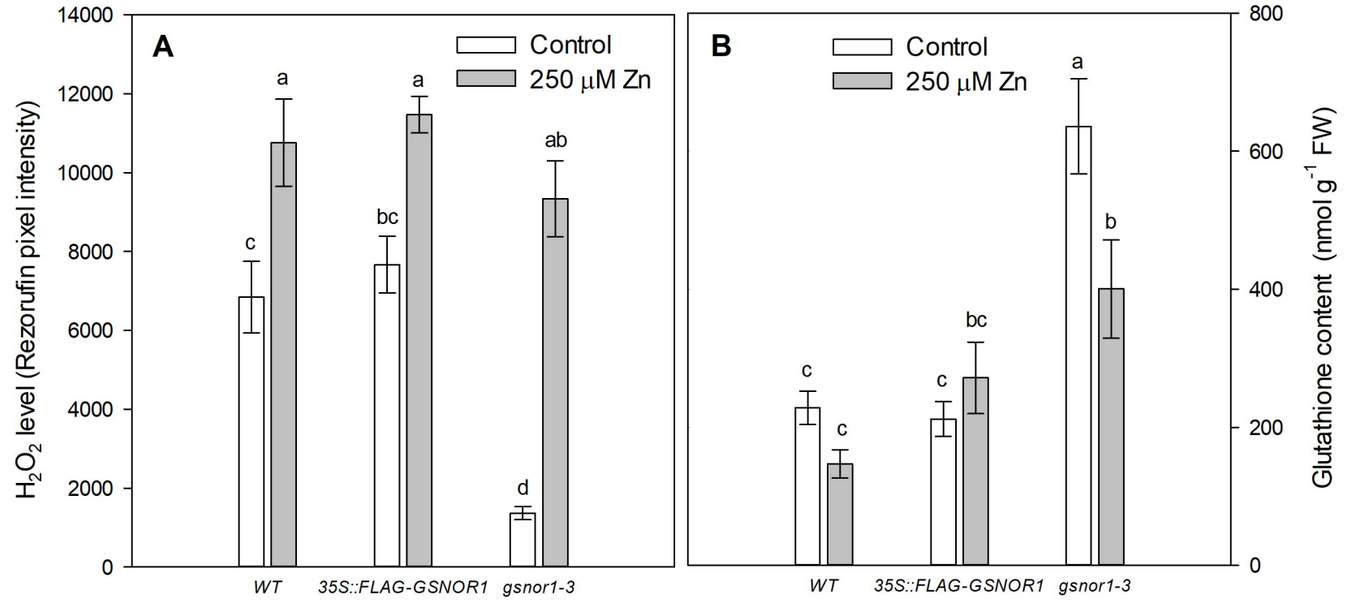
A
Control
250 μM Zn
$H_2O_2$ level (Rezorufin pixel intensity)
14000
12000
10000
8000
6000
4000
2000
0
c
a
bc
a
d
ab
WT
35S::FLAG-GSNOR1
gsnor1-3
B
Control
250 μM Zn
Glutathione content (nmol $g^{-1}$ FW)
800
600
400
200
0
c
c
c
bc
a
b
WT
35S::FLAG-GSNOR1
gsnor1-3

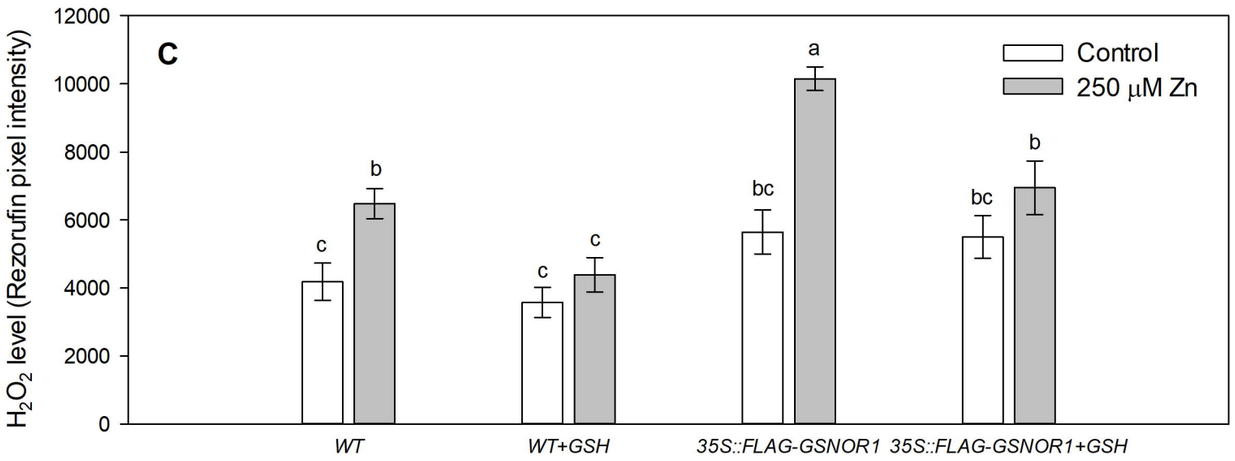
C
Control
250 μM Zn
$H_2O_2$ level (Rezorufin pixel intensity)
12000
10000
8000
6000
4000
2000
0
c
b
c
c
bc
a
bc
b
WT
WT+GSH
35S::FLAG-GSNOR1
35S::FLAG-GSNOR1+GSH

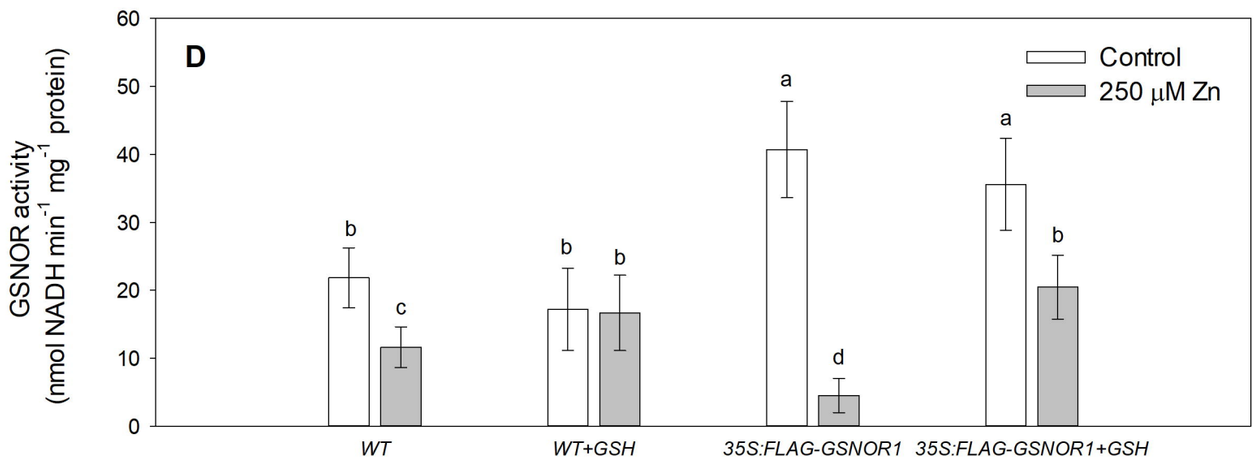
D
Control
250 μM Zn
GSNOR activity
(nmol NADH $min^{-1}$ $mg^{-1}$ protein)
60
50
40
30
20
10
0
b
c
b
b
a
d
a
b
WT
WT+GSH
35S:FLAG-GSNOR1
35S:FLAG-GSNOR1+GSH

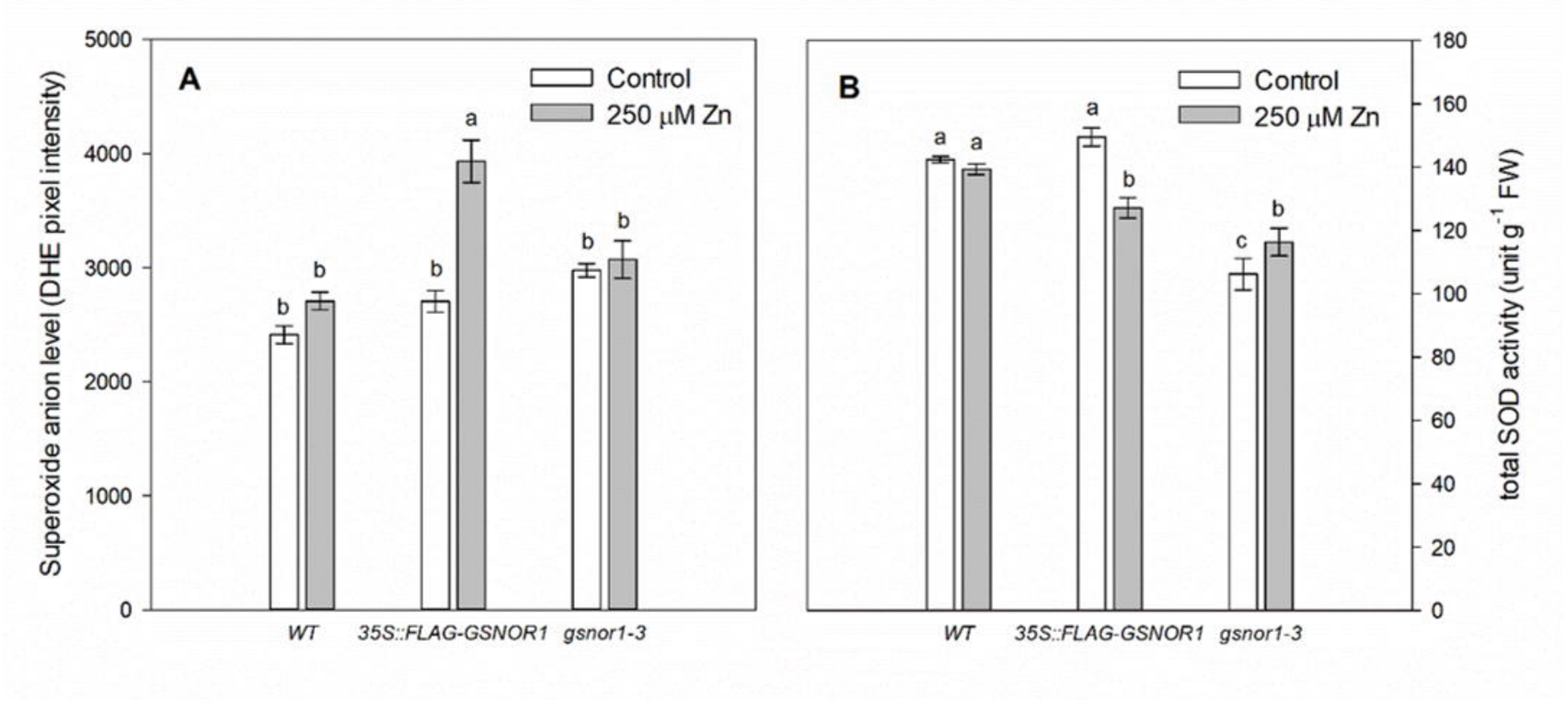
A
Control
250 μM Zn
Superoxide anion level (DHE pixel intensity)
5000
4000
3000
2000
1000
0
b
b
b
a
b
b
WT
35S::FLAG-GSNOR1
gsnor1-3
B
Control
250 μM Zn
total SOD activity (unit g-1 FW)
180
160
140
120
100
80
60
40
20
0
a
a
a
b
c
b
WT
35S::FLAG-GSNOR1
gsnor1-3

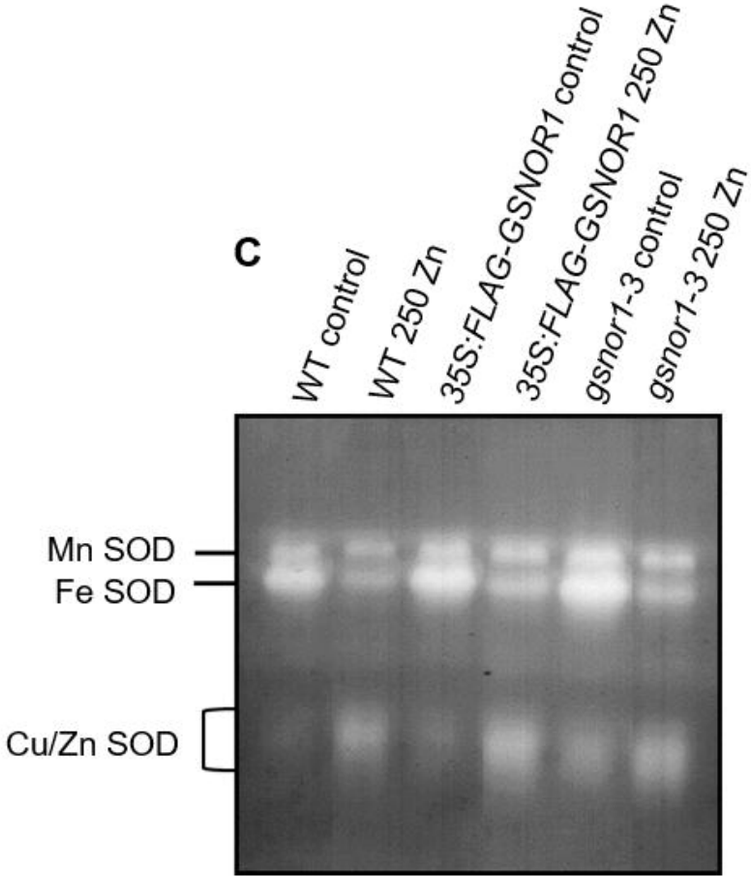
C
WT control
WT 250 Zn
35S:FLAG-GSNOR1 control
35S:FLAG-GSNOR1 250 Zn
gsnor1-3 control
gsnor1-3 250 Zn
Mn SOD
Fe SOD
Cu/Zn SOD

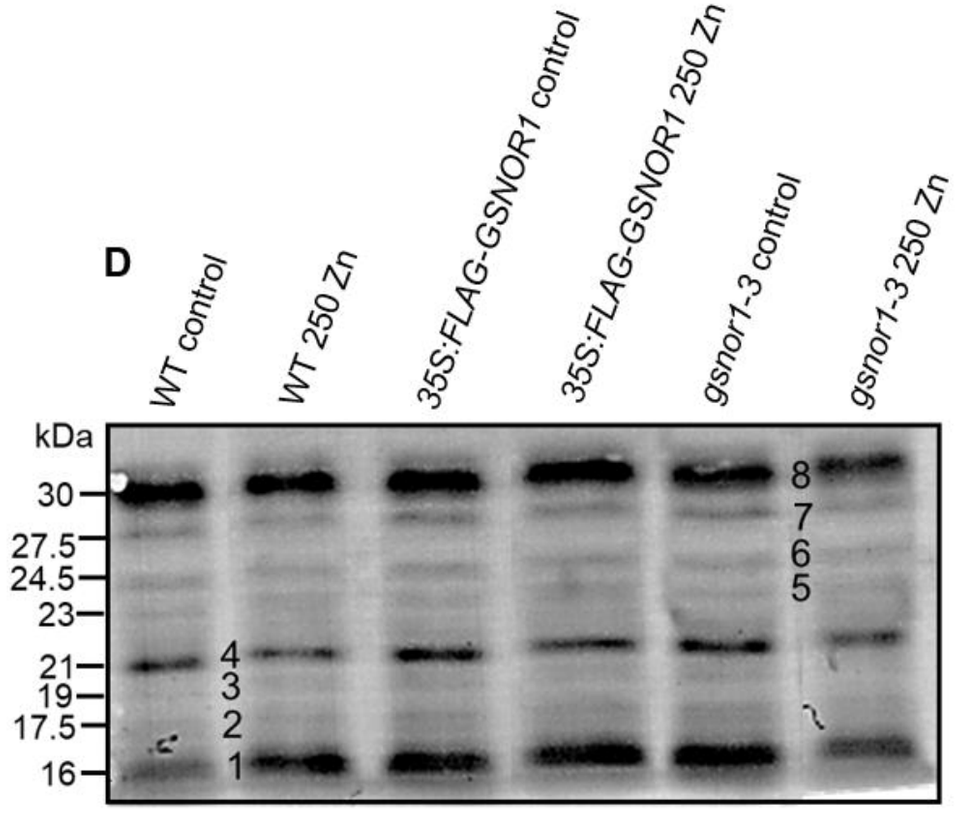
D
WT control
WT 250 Zn
35S:FLAG-GSNOR1 control
35S:FLAG-GSNOR1 250 Zn
gsnor1-3 control
gsnor1-3 250 Zn
kDa
30
27.5
24.5
23
21
19
17.5
16
1
2
3
4
5
6
7
8

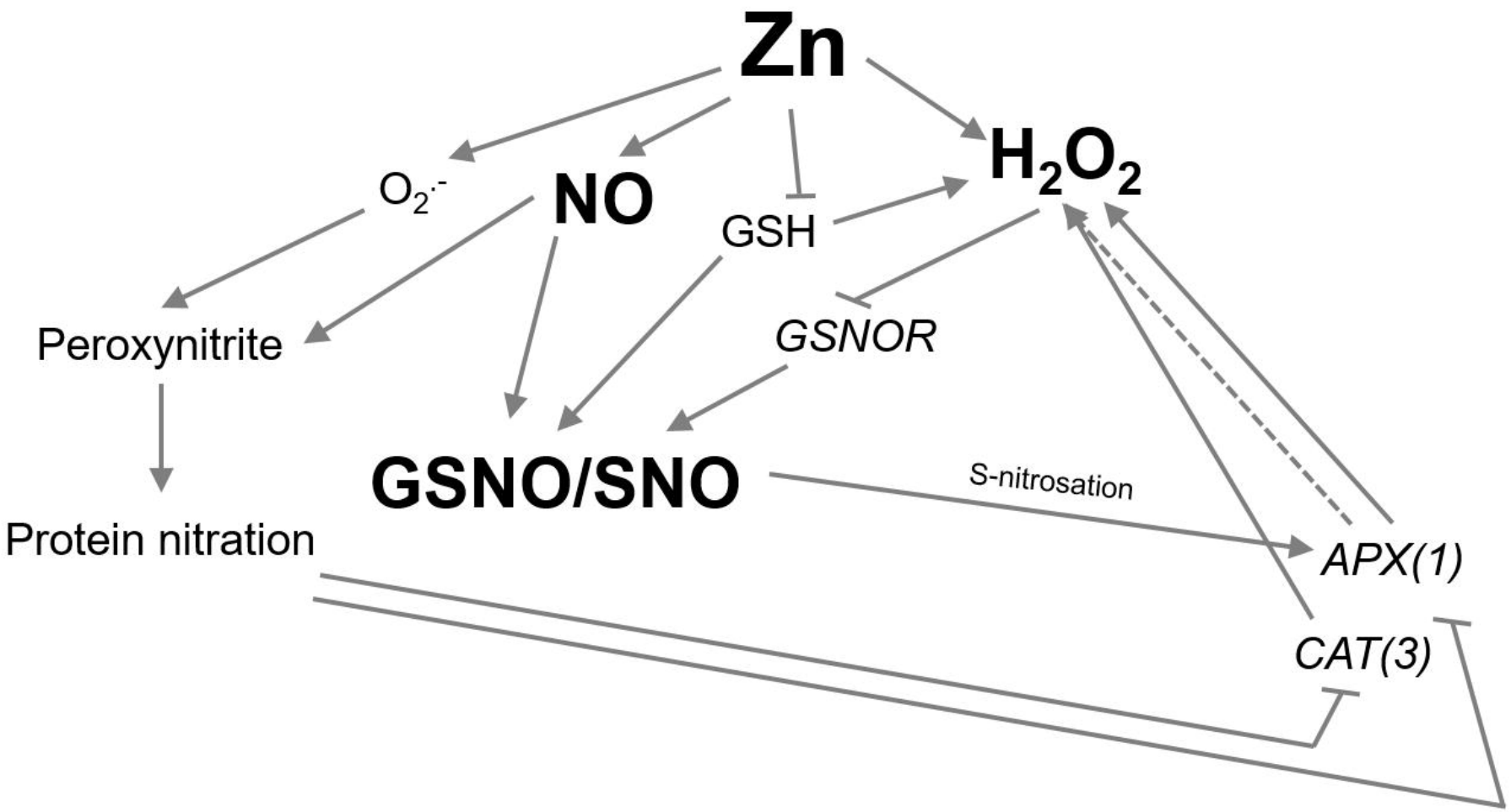
Zn
$O_2^{\cdot -}$
NO
GSH
$H_2O_2$
Peroxynitrite
GSNOR
GSNO/SNO
S-nitrosation
Protein nitration
APX(1)
CAT(3)